POLITECNICO DI TORINO

Master's Degree in Mechanical Engineering

Master's Degree Thesis

Parametric reduction techniques for the simulation of mistuning in bladed disks

Supervisors

Prof. Christian Maria Firrone
Dr. Giuseppe Battiato

Candidate

Francesco Battistoni

Academic Year 2021/2022

Abstract

In bladed disks' dynamics the so called "mistuning" is the effect of uncertainties which break the ideally tuned configuration imposed at the design stage.

Nowadays, the mistuning topic takes a great relevance in the turbomachinery field, since it is associated to a behaviour which is not predictable by analyses done with cyclic symmetry and leads to non conservative results in terms of peak amplitudes at resonance. From a numerical point of view, the study of mistuning requires the simulation of the whole bladed disk and consequently leads to high computational costs: for this purpose it is necessary to develop reduction techniques that must also take into account the perturbation of a design parameter.

This thesis focuses on the formulation of an effective parametric reduction technique in order to estimate the natural frequencies, the modeshapes and the forced response of structures characterized by a variation in one of their geometric parameters. Some specific methods, acting on the mass and stiffness matrices through an approach based on interpolation, are analyzed emphasizing the advantages and the drawbacks, especially when associated with a reduction technique as the Craig-Bampton CMS.

The application of the above mentioned methods starts from a simple one-dimensional MDOF system created in Matlab and then focuses on more complex models such as a 3D cantilever beam and a dummy blade, previously meshed in HyperMesh and then imported into ANSYS for the structural analysis.

Subsequently, the outcome of the thesis will be useful for the simulation of the dynamic behaviour of a bladed disk characterized by blades having different thickness.

Acknowledgements

Ci sono molte persone a cui vorrei porgere i miei ringraziamenti.

Partirò da coloro che mi hanno seguito, compreso e consigliato durante la stesura di questa tesi, ossia il Professor Christian Maria Firrone e il Dottor Giuseppe Battiato: senza il loro apporto non sarei riuscito a portare a termine questo lavoro e soprattutto non avrei appreso molte nozioni utili anche nell'ottica di un futuro impiego lavorativo.

Rimanendo in ambito universitario ci tengo molto a ringraziare i miei colleghi del team studentesco Eolito, con i quali negli scorsi anni ho condiviso dei bellissimi momenti di impegno e di divertimento.

Ringrazio poi la mia famiglia, in particolare i miei genitori, per essere stati comprensivi con me anche quando i miei atteggiamenti non erano del tutto favorevoli nei loro confronti.

Infine, un ulteriore ringraziamento va alla mia ragazza, Jessica, che ha sopportato la distanza, i miei silenzi e alcune mie scelte non sempre concilianti, ma che nonostante ciò non mi ha mai fatto mancare il suo supporto, soprattutto nei momenti più complicati.

Table of Contents

List of Figures

III

List of Tables

Introduction

1.1 Overview

Nowadays the study of turbomachines plays an important role in aviation industry, both civil and military, but also in the energy production sector. In the aeronautic field the target is to improve the performances, also in terms of emissions, while reducing the masses. The bladed disks represent one of the most critical components of these machines because they are rotating structures subjected to high load levels (static, dynamic and impact).
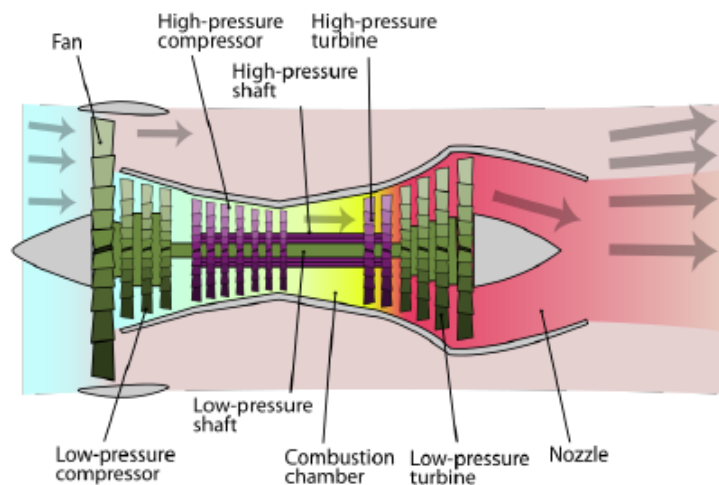
Figure 1.1: Schematic example of a Turbofan engine, [9]

In particular, the major problems encountered are connected to the High Cycle Fatigue (HCF), whose risks have to be mitigated in two possible ways: by avoiding dangerous resonances in the operating conditions (in general on the first modes), or accepting to encounter resonance in the frequency range exploited, because the associated response level has already been estimated during the design steps (check [4] for more details). The second approach is the most commonly used at industrial level since it is more economic with respect to performing expensive tests at the development stage. However, it also requires specific methods for the frequency

response function (FRF) computation. The computational cost of a 3D FEM model simulating a bladed disk composed by N blades is really high (millions of degrees of freedom). The structure cyclic symmetry property can be used to reduce the cost of the analysis by modelling only one blade and one disk portion, but it represents an ideal condition: indeed, bladed disks are never composed by identical sectors due to:

- manufacturing tolerances

- material's inhomogeneities

- assembling

- wear

- blades' damaging

All these inevitable differences are collectively called "Mistuning".

1.2 Mistuning

Due to the presence of mistuning, the results obtained from the modal analysis with cyclic symmetry and from the forced response with cyclic symmetry are not valid. The effects of mistuning on the bladed disks' dynamic behaviour are:

- splitting of the coupled modes

- modeshapes distortion

- higher vibration amplitudes in some blades

Without the cyclic symmetry the single sector cannot be used to realize the dynamic analyses and the whole model is necessary. Moreover, since the mistuning has a random nature, it is necessary to execute a large number of analysis to characterize the dynamic behaviour of the system by a statistical point of view. In literature two types of mistuning exist: the *small mistuning*, which is caused by manufacturing tolerances and wear, does not modify the single sector modeshapes, but only their amplitude of vibration; on the other hand the *large mistuning*, ascribable to events that deeply affect the blade's geometry (cracks, FOD), modify also the amplitude distribution between different blades.

At the design stage the focus in on the small mistuning, whose presence is identified through the variability of the blade natural frequencies. In fact, if all the blades were identical, they would have the same natural frequencies; because of the mistuning, different blades manifest different natural frequencies, even with same modeshapes. Therefore, it is common to model the small mistuning by changing the young modulus E or density ρ of the material used [9]. Another approach, that will be faced in this thesis work, is the modification of a single geometric parameter
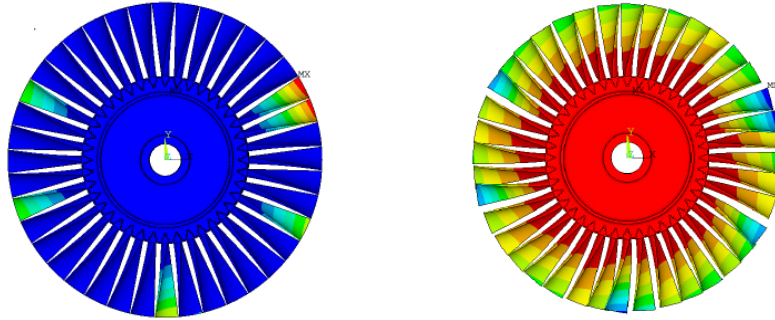
Figure 1.2: Small mistuning effect on bladed disk modeshapes, rigid disk (left), flexible disk (right) [9]

on the blade, for example the thickness of the main body, that affects its natural frequencies. In this way it will be possible to assemble a full bladed disk model characterized by slightly different blades. However, it is impossible to use the typical FEM full models for the dynamic analysis of a mistuned bladed disk. For this purpose it is convenient to develop reduced order models.

1.3 Craig-Bampton Component Mode Synthesis

The Craig-Bampton CMS is a reduction technique associated to a substructuring procedure. The degrees of freedom of each substructure can be divided into two sets: internal degrees of freedom and boundary degrees of freedom. The latter are all degrees of freedom that the substructure has in common with other parts of the structure, while the internal degrees of freedom are those belonging only to the relevant substructure. The largest reduction scheme is the one in which all internal degrees of freedom are considered slave coordinates and all boundary degrees of freedom are considered master coordinates. In this way however, the approximation can be quite rough: a simple way to avoid this drawback is to consider as master coordinates not only the boundary degrees of freedom but also some of the modal coordinates of the substructure constrained at its boundary. This procedure would obviously lead to exact results if all the modes were retained, but the computational advantages increase together with the number of modes that can be neglected [8]. The Craig-Bampton CMS method is expressed by the following mathematical passages, applied to a MDOF undamped model. The equation of motion in matrix form are represented below, where the vector $\{x_b\}$ represents the boundary degrees of freedom and the vector $\{x_i\}$ expresses the internal degrees of freedom.

$$[M]\{\ddot{x}\} + [K]\{x\} = \{0\} \tag{1.1}$$

$$\begin{bmatrix} [m_{bb}] & [m_{bi}] \\ [m_{ib}] & [m_{ii}] \end{bmatrix} \left\{ \begin{matrix} \{\ddot{x}_b\} \\ \{\ddot{x}_i\} \end{matrix} \right\} + \begin{bmatrix} [k_{bb}] & [k_{bi}] \\ [k_{ib}] & [k_{ii}] \end{bmatrix} \left\{ \begin{matrix} \{x_b\} \\ \{x_i\} \end{matrix} \right\} = \left\{ \begin{matrix} 0 \\ 0 \end{matrix} \right\} \tag{1.2}$$

It is important to notice that the mass matrix and the stiffness matrix are partitioned in order to satisfy the division between boundary and internal coordinates. By neglecting the effect of the inertia forces and considering the second set of equations we have:

$$[k_{ib}]\{x_b\} + [k_{ii}]\{x_i\} = \{0\} \tag{1.3}$$

$$\{x_i\} = -[k_{ii}]^{-1}[k_{ib}]\{x_b\} = [T]\{x_b\} \tag{1.4}$$

where $[T]$ is the static condensation matrix. In general, we call $\{y_i\}$ the second part of the response, which becomes:

$$\{x_i\} = [T]\{x_b\} + \{y_i\} \tag{1.5}$$

In matrix form we have:

$$\left\{ \begin{Bmatrix} \{x_b\} \\ \{x_i\} \end{Bmatrix} \right\} = \begin{bmatrix} [I] & [0] \\ [T] & [I] \end{bmatrix} \begin{Bmatrix} \{x_b\} \\ \{y_i\} \end{Bmatrix} \tag{1.6}$$

By substituting this result into the equations of motion we obtain:

$$\begin{bmatrix} [m_{bb}] & [m_{bi}] \\ [m_{ib}] & [m_{ii}] \end{bmatrix} \begin{bmatrix} [I] & [0] \\ [T] & [I] \end{bmatrix} \begin{Bmatrix} \{\ddot{x}_b\} \\ \{\ddot{y}_i\} \end{Bmatrix} + \begin{bmatrix} [k_{bb}] & [k_{bi}] \\ [k_{ib}] & [k_{ii}] \end{bmatrix} \begin{bmatrix} [I] & [0] \\ [T] & [I] \end{bmatrix} \begin{Bmatrix} \{x_b\} \\ \{y_i\} \end{Bmatrix} = \begin{Bmatrix} 0 \\ 0 \end{Bmatrix} \tag{1.7}$$

The second set of equations can be written as:

$$[m_{ib}]\{\ddot{x}_b\} + [m_{ii}][T]\{\ddot{x}_b\} + [m_{ii}]\{\ddot{y}_i\} + [k_{ib}]\{x_b\} + [k_{ii}][T]\{x_b\} + [k_{ii}]\{y_i\} = \{0\} \tag{1.8}$$

If we explicate the term $[T]$ the equation can be simplified to the following form:

$$[m_{ii}]\{\ddot{y}_i\} + [k_{ii}]\{y_i\} = (-[m_{ib}] - [m_{ii}][T])\{\ddot{x}_b\} \tag{1.9}$$

At first member we find the mass matrix and the stiffness matrix of the structure with $\{x_b\}$ equal to zero, which means that the structure is constrained at the boundary degrees of freedom, while at the second member we find the forces caused by the acceleration of the internal degrees of freedom. If we perform the eigenvalue problem of the latter, we'll have the following equations:

$$([k_{ii}] - \omega_{i,n}[m_{ii}])\{\Phi_i\}_n = 0 \tag{1.10}$$

$$\{y_i\} = [\Phi_i]\{q_i\} \tag{1.11}$$

$$\{x_i\} = [T]\{x_b\} + [\Phi_i]\{q_i\} \tag{1.12}$$

In matrix form we obtain:

$$\begin{Bmatrix} \{x_b\} \\ \{x_i\} \end{Bmatrix} = \begin{bmatrix} [I] & [0] \\ [T] & [I] \end{bmatrix} \begin{Bmatrix} \{x_b\} \\ \{y_i\} \end{Bmatrix} = \begin{bmatrix} [I] & [0] \\ [T] & [\Phi_i] \end{bmatrix} \begin{Bmatrix} \{x_b\} \\ \{q_i\} \end{Bmatrix} = [R] \begin{Bmatrix} \{x_b\} \\ \{q_i\} \end{Bmatrix} \tag{1.13}$$

where the matrix

$$[R] = \begin{bmatrix} [I] & [0] \\ [T] & [\Phi_i] \end{bmatrix} \tag{1.14}$$

is a rectangular matrix called "reduction matrix". As said before, the actual reduction lays in the fact that only some modes in the modal matrix of the internal degrees of freedom $[\Phi_i]$ are selected. Executing a pre and post multiplication of the full matrices by the reduction matrix, we obtain the reduced matrices, which are square matrices with a lower number of columns and rows with respect to the original full matrices.

$$[M][R] \begin{Bmatrix} \{\ddot{x}_b\} \\ \{\ddot{q}_i\} \end{Bmatrix} + [K][R] \begin{Bmatrix} \{x_b\} \\ \{q_i\} \end{Bmatrix} = \{0\} \tag{1.15}$$

$$[R]^T[M][R] \begin{Bmatrix} \{\ddot{x}_b\} \\ \{\ddot{q}_i\} \end{Bmatrix} + [R]^T[K][R] \begin{Bmatrix} \{x_b\} \\ \{q_i\} \end{Bmatrix} = \{0\} \tag{1.16}$$

$$[M_r] \begin{Bmatrix} \{\ddot{x}_b\} \\ \{\ddot{q}_i\} \end{Bmatrix} + [K_r] \begin{Bmatrix} \{x_b\} \\ \{q_i\} \end{Bmatrix} = \{0\} \tag{1.17}$$

In the end the matrices $[M_r]$ and $[K_r]$ will also show a peculiar partition: since the method takes into account the M-nomalized eigenvectors of the internal degrees of freedom $[\Phi_i]$, the resulting Craig-Bampton mass matrix $[M_r]$ will have the portion corresponding to the slave degrees of freedom equal to the identity matrix $[I]$, while the Craig-Bampton stiffness matrix $[K_r]$ will have the eigenvalues matrix $[\omega_n^2]$ in the same position.
This reduction technique is particularly useful when an assembly of more components or substructures needs to be studied: in bladed disks, the single blades are typically mounted around the disk by means of a dovetail geometry at the root, that constrains the radial displacements. In the same way, if the blades are shrouded, there will be also a constraint corresponding to a specific surface of the shroud. Both this constraints can be considered as interfaces between different substructures and this is the reason why the CB-CMS is really suitable for this type of components.

Methodology

2.1 Parametric reduced order models

The target of this thesis work is to associate the Craig-Bampton CMS technique with a parametric interpolation. In practice, this means to create a series of reduced order models, linked to a variation of one parameter, for example a geometric feature, into an interval of interest. Then, by means of specific techniques, a condition which does not corresponds to one of the reference reduced order models, but included into the above-mentioned interval, is going to be simulated and compared with the results coming from a full model created appositely for the validation. If the outcomes were successful, the advantages given by this procedure would be significant, since it would allow to avoid the performing of the reduction at every desired value of the parameter p. The method, from a theoretical point of view, is suitable for all the FEM systems that need to be reduced, in particular through the Craig-Bampton CMS, and that depend on one parameter variation. The principal industrial application that comes to mind in relation to what was explained before is the simulation of mistuning in bladed disks, since it is a phenomenon that modifies the natural frequencies and the modeshapes of the single blades and often need statistical analysis to carry out concrete results; if we think at the single blade as our model, the parametric reduction technique, once validated, would enable to create different mistuning patterns only selecting properly the value of the interpolated parameter, bypassing all the reduction's iterations.

For our case studies the choice has been to create 5 different equally spaced "stations", both for the more simple 1D models and for the more complex FEM models. The number of stations selected is not mandatory, but in some specific techniques can affect the degree of the interpolating polynomial, with consequences even on the percentage errors. In the following, the value p_0 represents the nominal parameter value, while Δp is the distance between two following stations. The main goal of the interpolation is to determine the mass and stiffness matrix of the reduced order model corresponding to a value of the parameter p included between the extremes. In addition, the parameter vector's elements have been chosen according to the model treated, but in general the criterion has been the evaluation of the percentage variation of the natural frequencies computed at the different stations: it is evident that the larger is the interval between two consecutive stations, the less accurate will be the results of the interpolation used.

The five station of the varying parameter can be represented in a vector form as below:

$$p_{vect} = [p_0 - 2\Delta p, \ p_0 - \Delta p, \ p_0, \ p_0 + \Delta p, \ p_0 + 2\Delta p] \tag{2.1}$$

The parametric interpolation techniques present in literature are various, but we'll focus only on three of them, which are the most easy to implement: the first one was inspired by the analyses of Epureanu et al [1] about the approximation of the mass and stiffness matrices of peculiar systems by means of the Taylor series approximation. The other two techniques were conceived appositely for this thesis work and act on the mass and stiffness matrices or on the modal and eigenvalues matrices by means of a polynomial interpolation. The above-mentioned techniques will be now presented describing the theory aspects on which they rest on, then in the following chapters they'll be applied to different type of models in order to highlight advantages and drawbacks of each of them. The study will be carried out with a special attention on the results provided in terms of natural frequencies, linear forced response and MAC computation with respect to a reference analytic or FEM model.

2.2 Taylor series finite differences method

The first procedure studied is based on the fact that the modification of the stiffness matrix due to variations in the thickness can be accurately represented by a Taylor series up to the third order, while the mass matrix can be approximated by a Taylor series up to first order, neglecting the rotary inertia [1]. The first and third order Taylor series approximations around the nominal parameter value p_0 can be expressed as follows:

$$\mathbf{M}(p) \approx \mathbf{M}(p_0) + \frac{\partial \mathbf{M}}{\partial p}(p - p_0) \tag{2.2}$$

$$\mathbf{K}(p) \approx \mathbf{K}(p_0) + \frac{\partial \mathbf{K}}{\partial p}(p - p_0) + \frac{1}{2}\frac{\partial^2 \mathbf{K}}{\partial p^2}(p - p_0)^2 + \frac{1}{6}\frac{\partial^3 \mathbf{K}}{\partial p^3}(p - p_0)^3 \tag{2.3}$$

The partial derivatives can be approximated using finite differences for a small parameter variation Δp as indicated in the next equations:

$$\mathbf{M}_{FD}^1 = \frac{\partial \mathbf{M}}{\partial p} \approx \frac{\mathbf{M}(p_0 + \Delta p) - \mathbf{M}(p_0)}{\Delta p} \tag{2.4}$$

$$\mathbf{K}_{FD}^1 = \frac{\partial \mathbf{K}}{\partial p} \approx \frac{\mathbf{K}(p_0 + \Delta p) - \mathbf{K}(p_0)}{\Delta p} \tag{2.5}$$

$$\mathbf{K}_{FD}^2 = \frac{\partial^2 \mathbf{K}}{\partial p^2} \approx \frac{1}{2}\frac{\mathbf{K}(p_0 + \Delta p) - 2\mathbf{K}(p_0) + \mathbf{K}(p_0 - \Delta p)}{\Delta p^2} \tag{2.6}$$

$$\mathbf{K}_{FD}^3 = \frac{\partial^3 \mathbf{K}}{\partial p^3} \approx \frac{\mathbf{K}(p_0 + 2\Delta p) - 3\mathbf{K}(p_0 + \Delta p) + 3\mathbf{K}(p_0) - \mathbf{K}(p_0 - \Delta p)}{\Delta p^3} \tag{2.7}$$

Subsequently, the parameterized matrices can be obtained by substituting the finite differences terms into the Taylor series approximations:

$$\mathbf{M}(p) \approx \mathbf{M}(p_0) + \mathbf{M}_{FD}^1 (p - p_0) \tag{2.8}$$

$$\mathbf{K}(p) \approx \mathbf{K}(p_0) + \mathbf{K}_{FD}^1 (p - p_0) + \frac{1}{2}\mathbf{K}_{FD}^2 (p - p_0)^2 + \frac{1}{6}\mathbf{K}_{FD}^3 (p - p_0)^3 \tag{2.9}$$

Another possible solution, as stated in [2], is the approximation of the stiffness matrix by means of a second order Taylor series, while the variation of the mass matrix is not taken into account. It follows that:

$$\mathbf{M}(p) \approx \mathbf{M}(p_0) \tag{2.10}$$

$$\mathbf{K}(p) \approx \mathbf{K}(p_0) + \frac{\partial \mathbf{K}}{\partial p}(p - p_0) + \frac{1}{2}\frac{\partial^2 \mathbf{K}}{\partial p^2}(p - p_0)^2 \tag{2.11}$$

with the approximations of the first and second order finite differences given by

$$\mathbf{K}_{FD}^1 = \frac{\partial \mathbf{K}}{\partial p} \approx \frac{-\mathbf{K}(p_0 + 2\Delta p) + 4\mathbf{K}(p_0 + \Delta p) - 3\mathbf{K}(p_0)}{2\Delta p} \tag{2.12}$$

$$\mathbf{K}_{FD}^2 = \frac{\partial^2 \mathbf{K}}{\partial p^2} \approx \frac{\mathbf{K}(p_0 + 2\Delta p) - 2\mathbf{K}(p_0 + \Delta p) + \mathbf{K}(p_0)}{\Delta p^2} \tag{2.13}$$

These two approaches are clearly similar from a conceptual point of view and differs only by the Taylor series order and finite differences terms.

2.3   Element by element interpolation

The most basic procedure is the one that iterates the interpolation on each element of the mass and stiffness matrix. The interpolation in general will be of polynomial type, with the polynomial order depending on the number of stations used: for example with four stations the polynomial order will be equal to three and a linear interpolation will be generated if the stations considered are only two. Clearly, this is not the most convenient way to obtain the interpolated matrices, especially from a computational point of view, but it is also a really general method which does not take care of the specific application of the problem. Another important aspect to

underline is that, treating linear systems, the mass and stiffness matrices expected at the end of the interpolation must respect the symmetry property: this means that is possible to limit the procedure to the upper triangular or the lower triangular part of the matrices and to put them back together by an overturn. In addition, the interpolation is performed into the software Matlab by means of the functions *polyfit* and *polyval*.

2.4 Interpolation of eigenvalues and eigenvectors

The last procedure examined does not act directly on the mass and stiffness matrices, but realizes an interpolation between the eigenvalues and eigenvectors of the single stations. Firstly the Craig-Bampton mass and stiffness matrices of each station are used to compute the eigenvalues and the eigenvectors matrices as follows:

$$([K_s] - \omega_{s,n}[M_s])\{\Phi_s\}_n = 0 \tag{2.14}$$

where the subscript s indicates the number of the station considered. The eigenvalues matrix $[D_s]$ is diagonal and contains the square values of the natural frequencies,

$$[D_s] = \begin{bmatrix} \omega_{s,1}^2 & & & & \\ & \ddots & & & \\ & & \omega_{s,i}^2 & & \\ & & & \ddots & \\ & & & & \omega_{s,N}^2 \end{bmatrix} \tag{2.15}$$

while the eigenvectors matrix $[\Phi_s]$ (also called modal matrix) contains the mode-shapes of the reduced order model. In further detail the modes are placed along the columns, the first rows are associated to the master degrees of freedom and the last rows to the slave degrees of freedom, as a consequence of the Craig-Bampton CMS reduction. Before performing the interpolation, the modal matrices must be arranged properly: this means that the eigenvectors sign of the physical displacements must be consistent between different stations, so it is needed a sign check for every mode with respect to its corresponding at the nominal station. At this point the interpolation can be performed: it is an operation which is quite expensive from a computational point of view, especially for the eigenvectors matrix, because it acts on its single cells (the modal matrices $[\Phi_s]$ are not symmetric so all their elements must be processed). In the end a new eigenvalues matrix $[D_p]$ and a new eigenvectors matrix $[\Phi_p]$ in correspondence of the selected parameter p are obtained. In order to be coherent with the other methods described, the aim of this procedure is to determine the mass matrix $[M_p]$ and the stiffness matrix $[K_p]$ at the interpolated condition; for this purpose it is possible to exploit the property of M-orthogonality

and K-orthogonality of the eigenvectors, which in this case are also M-normalized. Therefore, the mass modal matrix and the stiffness modal matrix are

$$[M_{p,mod}] = [\Phi_p]^T[M_p][\Phi_p] = [I] \tag{2.16}$$

$$[K_{p,mod}] = [\Phi_p]^T[K_p][\Phi_p] = [D_p] \tag{2.17}$$

If we perform the inverse operation we can go back to the mass and stiffness matrices as follows:

$$[M_p] = ([\Phi_p]^T)^{-1}[I]([\Phi_p])^{-1} \tag{2.18}$$

$$[K_p] = ([\Phi_p]^T)^{-1}[D_p]([\Phi_p])^{-1} \tag{2.19}$$

Finally, in order to ensure that the two interpolated matrices are symmetrical and so avoid numerical errors, some other passages can be done in Matlab

$$[\tilde{M}_p] = \frac{1}{2}(triu([M_p]) + tril([M_p]^T)) \tag{2.20}$$

$$[M_p] = [\tilde{M}_p] + [\tilde{M}_p]^T - diag(diag([\tilde{M}_p])) \tag{2.21}$$

In a similar way,

$$[\tilde{K}_p] = \frac{1}{2}(triu([K_p]) + tril([K_p]^T)) \tag{2.22}$$

$$[K_p] = [\tilde{K}_p] + [\tilde{K}_p]^T - diag(diag([\tilde{K}_p])) \tag{2.23}$$

where the commands *triu* and *tril* indicates respectively the upper triangular part and the lower triangular part of the matrix while *diag* extracts its main diagonal.

2.5 Results computation

The comparison bewtween interpolated and reference models will focus on three main aspects: natural frequencies, Modal Assurance Criterion (MAC), and linear forced response. For this purpose it is useful to resume these theoretical aspects from an analytical point of view. The natural frequencies of the system are computed from the eigenvalue problem (EVP): this operation is performed directly in Matlab by means of the function *eig* acting on the matrices $[M]$ and $[K]$. The percentage error on the natural frequencies is always computed in the following way:

$$error = 100 \cdot (freq_p - freq_{ref})/freq_{ref} \tag{2.24}$$

where the subscript p indicates the interpolated condition, while the subscript ref stands for reference.

On the other hand, the modal assurance criterion, typically called MAC is a powerful tool of comparison between eigenvectors, as demonstrated by its formulation:

$$MAC(i,j) = \frac{|\{\phi_A\}_i{}^T\{\phi_B\}_j|^2}{(\{\phi_A\}_i{}^T\{\phi_A\}_i)(\{\phi_B\}_j{}^T\{\phi_B\}_j)} \tag{2.25}$$

The subscripts i, j refers to the modeshape taken into account, while the subscripts A, B are associated to the different type of eigenvectors estimation. For example in this thesis the comparison will be often realized between the eigenvectors coming from the interpolation method and the ones coming from the FEM software or the analytical model. The indications that the MAC provides are fundamental: in fact, when the same modeshape computed with different procedures is selected ($MAC(i,i)$), if the MAC tends to 1 it means that the two eigenvectors are really similar to each other and it is also a proof of quality for the estimation. In all the other conditions the MAC is not predictable, but it should be much lower than 1. In matrix form the MAC computation should give high values (close to 1) along the main diagonal, and lower values tending to 0 in all the other positions.

For what concerns the forced response, many different approaches are possible: the easiest one, that is also the most expensive computationally, consist in the dynamic stiffness matrix inversion. Starting from the equations of motion of a MDOF system, it is possible to define the dynamic stiffness matrix as follows

$$[M]\{\ddot{x}\} + [C]\{\dot{x}\} + [K]\{x\} = \{f\} \tag{2.26}$$

$$\left(-\omega^2[M] + i\omega[C] + [K]\right)\{X\}e^{i\omega t} = \{F\}e^{i\omega t} \tag{2.27}$$

$$[K_{dyn}] = \left(-\omega^2[M] + i\omega[C] + [K]\right) \tag{2.28}$$

$$[K_{dyn}]\{X\} = \{F\} \tag{2.29}$$

Through an inversion of the dynamic stiffness matrix the forced response can be easily computed for many values of frequency ω.

$$\{X\} = [K_{dyn}]^{-1}\{F\} \tag{2.30}$$

It is important also to point out that neglecting the inertia and damping terms the static response can be obtained

$$\{X\} = [K]^{-1}\{F\} \tag{2.31}$$

The damping matrix deserves a deepening because it is not directly derived from the model. Initially a damping factor ζ has to be set, that typically in simulation activities is the same for all modes. Then the modal damping matrix is consequently determined

$$[C_{mod}] = diag(2\zeta\omega_n) \tag{2.32}$$

However, from the definition of modal damping matrix we can also write

$$[C_{mod}] = [\Phi]^T[C][\Phi] \tag{2.33}$$

and by an inverse operation we finally obtain the damping matrix

$$[C] = ([\Phi]^T)^{-1}[C_{mod}][\Phi]^{-1} \tag{2.34}$$

Another approach that is frequently employed to compute the linear forced response is based on the mode superposition formulation

$$\{X\} = \sum_{n=1}^{Q} \frac{\{\phi_n\}^T\{F\}\{\phi_n\}}{\omega_n^2 - \omega^2 + i2\zeta\omega_n\omega} \tag{2.35}$$

In order to plot the FRF it is clear that the operation must be repeated for every step of frequency. Moreover, for sake of simplicity, the forcing vector will have only one element different from zero: this means that the force will be applied in correspondence of a specific degree of freedom and the same can be said for the detection of the displacement. The advantage of this second procedure is that only few modes (Q < N) can be used to obtain the forced response, while in the previous case the inversion of the whole dynamic stiffness matrix included all the modes.

Applications

3.1 One-dimensional model

The preliminary analyses have been conducted over an extremely simple model, constituted by a series of alternating spring and mass elements as represented in the figure below
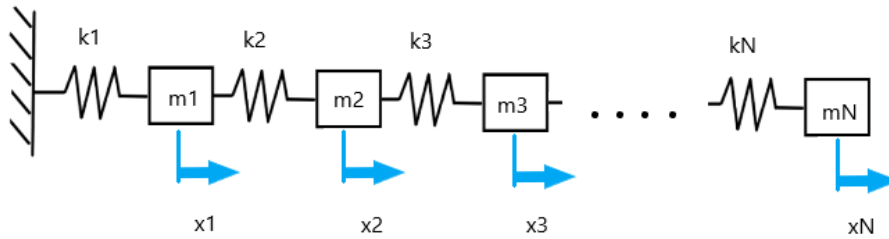
Figure 3.1: Schematic representation of the 1D MDOF system

The resulting multi-degrees of freedom system is characterized by N elements, the first clamped and the last corresponding to a free end. The degrees of freedom are clearly defined by only one coordinate and have positive direction towards the free end of the system. The mass and stiffness matrices of the whole model are represented by a diagonal and a tridiagonal matrix respectively. For sake of simplicity all the masses have been considered equal to each other and the same is also valid for the stiffness' values, so that the full matrices can be written quickly as follows

$$[M] = m \cdot [I] \tag{3.1}$$

$$[K] = k \cdot \begin{bmatrix} 2 & -1 & & & & \\ -1 & 2 & -1 & & & \\ & & \ddots & \ddots & \ddots & \\ & & & -1 & 2 & -1 \\ & & & & -1 & 1 \end{bmatrix} \tag{3.2}$$

In this model the five stations could not be associated to a particular geometry feature variation, so that some assumptions about the trend of stiffness and mass along the stations had to be made. In particular, the choice was to impose a quadratic law of variation for the stiffness and a linear law of variation for the mass. In tabular form the situation is represented by the following set of data,

Station N°	1	2	3	4	5
parameter p [-]	-2	-1	0	1	2
m [kg]	2.6	2.8	3	3.2	3.4
k [N/m]	$1.05 \cdot 10^6$	$1.05 \cdot 10^6$	$1.05 \cdot 10^6$	$1.05 \cdot 10^6$	$1.05 \cdot 10^6$

Table 3.1: Mass and stiffness values along the 5 stations

while from a graphical point of view the trend of variation is shown in the diagrams below
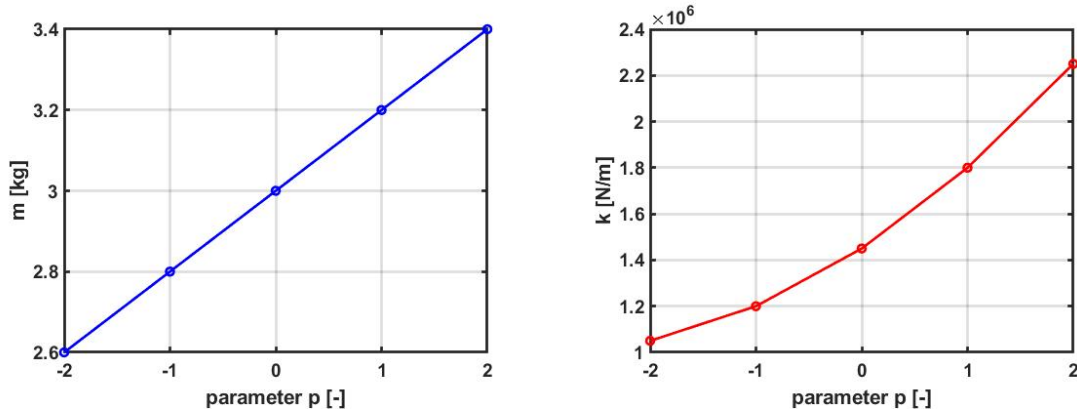
Figure 3.2: Mass and stiffness variation along the 5 stations

The selection of these set of values in terms of mass and stiffness was determined by the desire to obtain a variation of the first natural frequency included between -10% and $+10\%$ with respect to the station at the nominal parameter (3rd station). These hypothesis have been been considered valid both for the full 1D model and for the reduced order 1D model, as explained in the next paragraphs.

3.1.1 Full model

As a first basic step, the various interpolation approaches have been tested on a full model composed by 50 mass elements and 50 stiffness elements: this means that no reduction was performed at this stage. The reference condition with respect to which the results were compared has been represented by a specific value of the parameter p so that the mass value was equal to 2.64 kg and the stiffness value was equal to $1.144 \cdot 10^6$ N/m. It is important to underline the fact that this values are included into the interval defined by the extreme stations, but also that they are not

corresponding to one of them. The first 10 natural frequencies of the five stations are listed in table 3.2.

Mode	freq S1 [Hz]	freq S2 [Hz]	freq S3 [Hz]	freq S4 [Hz]	freq S5 [Hz]
1	3.15	3.24	3.44	3.71	4.03
2	9.43	9.72	10.32	11.13	12.08
3	15.71	16.18	17.19	18.55	20.11
4	21.98	22.64	24.04	25.94	28.13
5	28.22	29.07	30.87	33.31	36.12
6	34.44	35.47	37.67	40.64	44.08
7	40.62	41.84	44.44	47.94	51.99
8	46.76	48.17	51.16	55.19	59.86
9	52.86	54.45	57.83	62.39	67.66
10	58.91	60.68	64.44	69.52	75.40

Table 3.2: Natural frequencies at the 5 stations, 1D full model

It is possible to notice that the natural frequencies grow gradually along the stations and this means that the quadratic variation of the stiffness has a major impact with the respect to the linear variation of the mass. In the next paragraphs we'll refer to the interpolated condition with the acronym *PROM* (Parametric Reduced Order Model), even if in this first discussion no reduction has been performed.

Taylor series finite differences method

We start presenting the results associated to the Taylor series interpolation, with derivatives approximated by means of finite differences terms according to the Epureanu et al.[1] approach. Taking into account only the first 10 modes, the results in terms of natural frequencies are exposed in the following table

Mode	PROM frequency [Hz]	Test frequency [Hz]	Percentage error [%]
1	3.17	3.15	0.64
2	9.50	9.46	0.42
3	15.82	15.76	0.38
4	22.13	22.04	0.41
5	28.42	28.30	0.42
6	34.68	34.53	0.43
7	40.90	40.73	0.42
8	47.09	46.89	0.43
9	53.23	53.01	0.41
10	59.32	59.07	0.42

Table 3.3: Natural frequencies comparison, 1D full model, Taylor series interpolation with finite differences (Epureanu et al.[1]) VS analytical model

The approximation obtained by the interpolation is quite good in terms of natural frequency, since the percentage error is lower than 1% for every mode and tends to

settle about the 0.4%. Even the MAC computation gives a really positive result, which means that the eigenvectors of the two compared models are almost identical. This fact can be evinced by the following image, where the diagonal elements of the MAC matrix tends to 1, while in all the other position the correlation does not exist and the values fall towards zero.
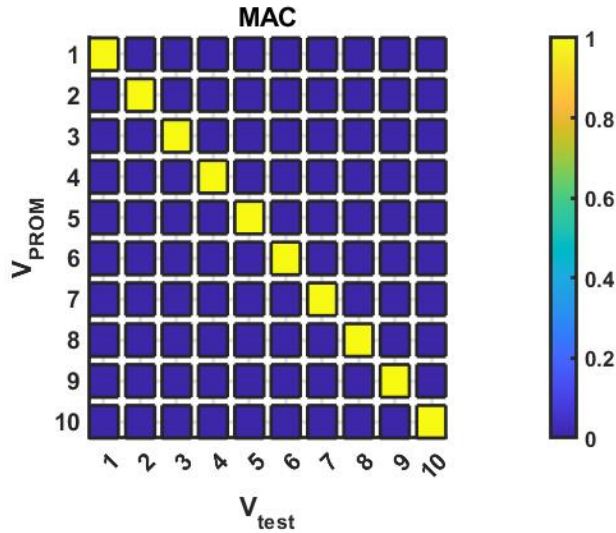
Figure 3.3: MAC, 1D full model, Taylor series interpolation with finite differences (Epureanu et al.[1]) VS analytical model

In addition it is interesting to plot also a couple of modeshapes, in order to corroborate the eigenvectors comparison. In figures 3.4 and 3.5 are reported the relative displacements of the 2nd and the 5th eigenvectors of the system: it is evident that the *PROM* condition represented by the red dots follows in a perfect way the deformed shape of the reference condition (in blue) for both modes. It is also advisable to remember that the system is constrained at the left end, while it is free at the right end, as showed by the relative displacement corresponding to the 0 and 50 value on the x axis respectively.

For what concerns the forced response, in figures 3.6 and 3.7 it is reported its trend in a frequency range selected specifically to highlight the resonance at the first mode. The damping factor has been set as $\zeta = 0.02$, the force was applied to the 34th degree of freedom, with an intensity of 1 N, while the displacement amplitude has been detected at the 38th degree of freedom; moreover, the frequency vector has been discretized with 500 elements. The computation has been performed both with the inversion of dynamic stiffness matrix approach and with the mode superposition approach, employing in this second case only 5 modes. The two images are practically the same and this demonstrates that the two methods are equivalent; however, the second approach allows to use less modes for the calculus and as a consequence it is also less expensive computationally. For this reason from now on the mode superposition method has been preferred even for the application to more complex models.
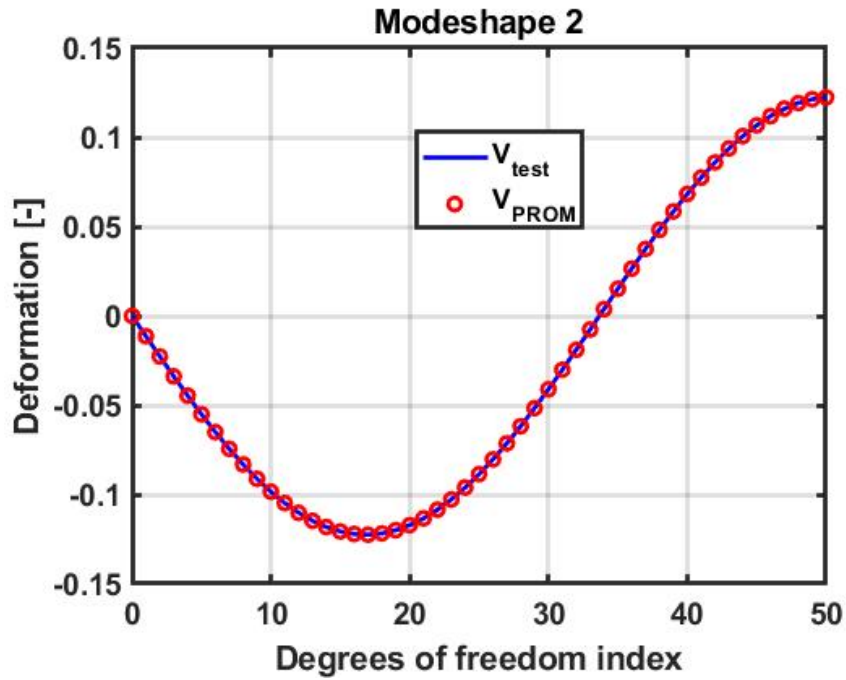
Figure 3.4: Modeshape 2, 1D full model, Taylor series interpolation with finite differences (Epureanu et al.[1]) VS analytical model
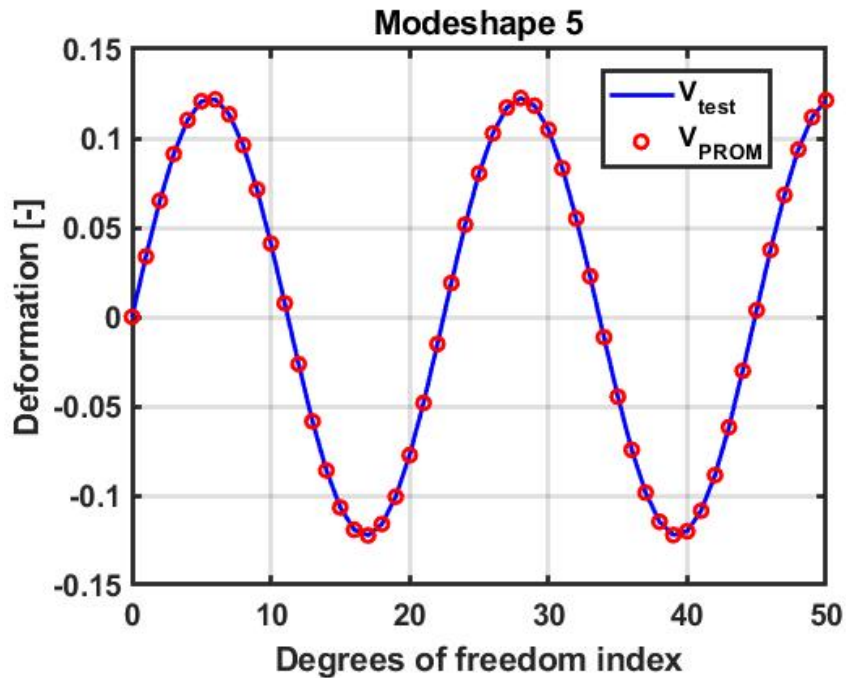
Figure 3.5: Modeshape 5, 1D full model, Taylor series interpolation with finite differences (Epureanu et al.[1]) VS analytical model
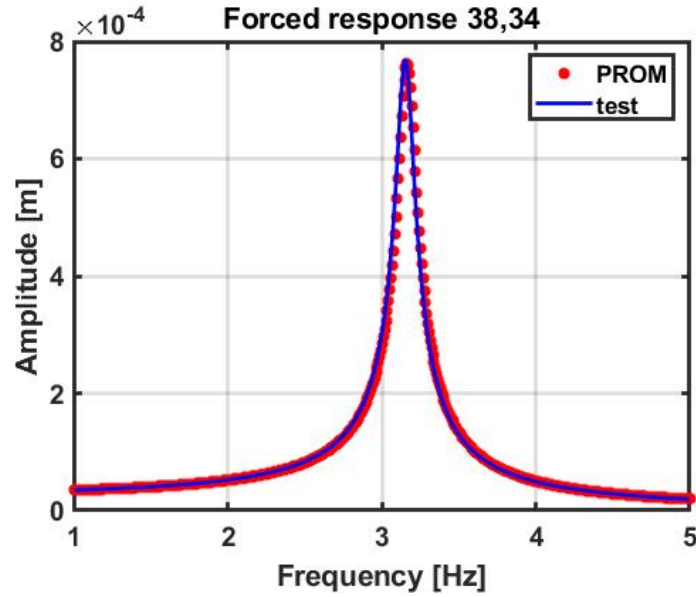
Figure 3.6: Forced response computed by means of $[K_{dyn}]$ inversion, 1D full model, Taylor series interpolation with finite differences (Epureanu et al.[1]) VS analytical model
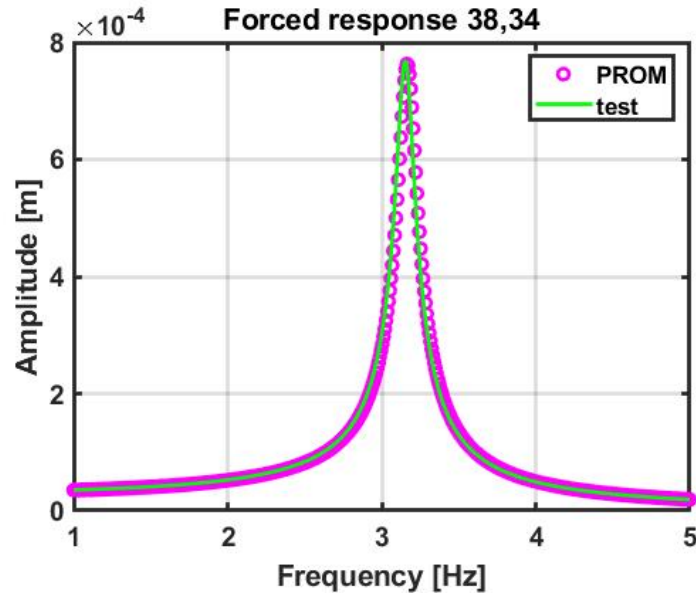
Figure 3.7: Forced response computed by means the mode superposition, 1D full model, Taylor series interpolation with finite differences (Epureanu et al.[1]) VS analytical model

If we consider now the same procedure applied above, but for the Taylor series with the derivatives approximated by means of finite differences terms according to

the Kurstak et al.[2] approach, we obtain the results listed in table 3.4.

Mode	PROM frequency [Hz]	Test frequency [Hz]	Percentage error [%]
1	2.96	3.15	-6.03
2	8.87	9.46	-6.24
3	14.78	15.76	-6.24
4	20.67	22.04	-6.24
5	26.55	28.30	-6.18
6	32.39	34.53	-6.20
7	38.21	40.73	-6.19
8	43.99	46.89	-6.18
9	49.72	53.01	-6.21
10	55.41	59.07	-6.20

Table 3.4: Natural frequencies comparison, 1D full model, Taylor series interpolation with finite differences (Kurstak et al.[2]) VS analytical model

It can be seen easily that the percentage errors are much higher than the previous case, surely because with this second approach the interpolated mass matrix does not show any variation with respect to the nominal one: this fact implies that the natural frequencies obtained are lower than the reference ones. With regard to the MAC, the result is the same as the previous one and this means that the eigenvectors comparison keeps on giving good results, independently from the error on the natural frequencies. This discrepancy becomes evident in the diagram of the forced response, where the peak of the interpolated response is shifted towards left with respect to the reference peak.
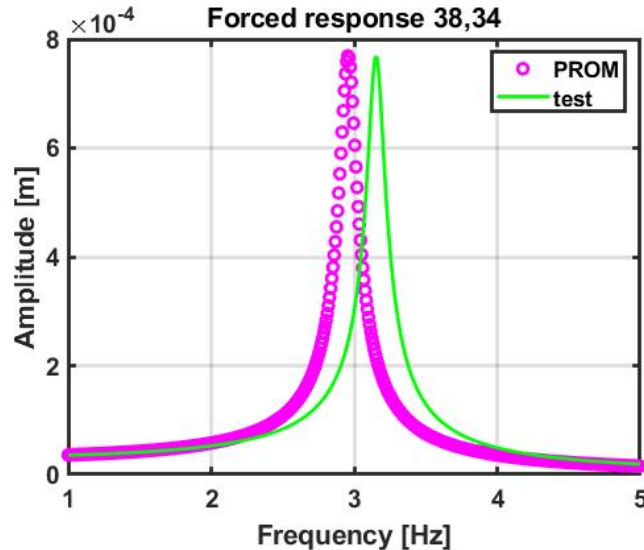
Figure 3.8: Forced response, 1D full model, Taylor series interpolation with finite differences (Kurstak et al.[2]) VS analytical model

Element by element interpolation

Using this type of interpolation, the results are really similar to the ones obtained before by means of the Taylor series with Epureanu et al.[1] finite differences approximation, especially in terms of MAC and forced response. In order to avoid redundancies, the concerning figures are not shown in this section, while the percentage errors of the natural frequencies, neglecting numerical errors, are equal to zero, as shown in table 3.5. This happens because the degree of the interpolating polynomial for each element of the mass and stiffness matrices between the 5 stations is higher with respect to the degree of variation of the mass (linear) and stiffness (quadratic) employed for the analytical reference model.

Mode	PROM frequency [Hz]	Test frequency [Hz]	Percentage error [%]
1	3.15	3.15	0.00
2	9.46	9.46	0.00
3	15.76	15.76	0.00
4	22.04	22.04	0.00
5	28.30	28.30	0.00
6	34.53	34.53	0.00
7	40.73	40.73	0.00
8	46.89	46.89	0.00
9	53.01	53.01	0.00
10	59.07	59.07	0.00

Table 3.5: Natural frequencies comparison, 1D full model, Element by element interpolation VS analytical model

One aspects that it is worth to add is about the forced response: if we want to plot the response of the system over a range of frequency that includes more than one mode, the mode superposition method can be misleading when set with a number of modes lower than the number of modes present in that frequency interval. For example, by keeping the same damping factor, force application degree of freedom and displacement detection degree of freedom of the previous cases, but expanding the frequency range between 1 Hz and 50 Hz, by means of the dynamic stiffness matrix inversion approach we can notice 8 peaks of resonance, while the mode superposition method with 5 modes selected will be able to highlight only the resonances associated to them. The situation is clearly represented in figure 3.9.

Interpolation of eigenvalues and eigenvectors

Trough the interpolation of eigenvalues and eigenvectors the results are absolutely similar to the ones described in the element by element section, both in terms of natural frequencies percentage errors, which tend to zero, and also looking at the MAC and forced response diagrams (not reported for brevity).
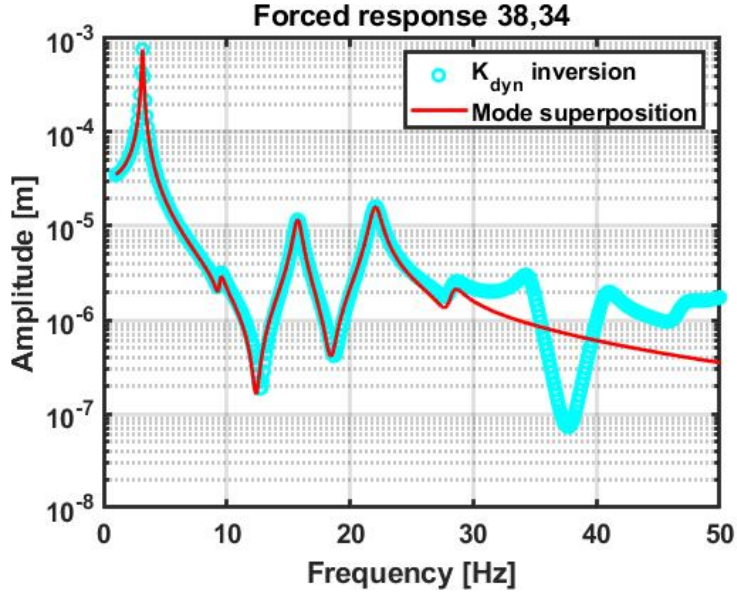
Figure 3.9: Forced response, 1D full model, Element by element interpolation, $[K_{dyn}]$ inversion VS Mode superposition

In summary, the analysis of the different parametric interpolation methods on the full 1D model provided really good results for what concerns the approximation of natural frequencies, modeshapes and forced response computation. Moreover, the matrix conformation between the stations' matrices and the interpolated matrices is preserved, a condition that is not automatically respected as we'll see in the next chapters. In general, the procedures based on the interpolation of the stiffness and mass matrices elements and on the interpolation of eigenvalues and eigenvectors provided lower percentage errors with respect to the others, while in terms of forced response and MAC computation the results were almost identical. For what concerns the Taylor series approaches, the Epureanu et al.[1] approximation showed better outcomes compared to the Kurstak et al.[1] one: in the latter, the mass variation along the parameter was not taken into account, with a consequent underestimation of the natural frequencies about the reference. Since the following more complex 3D models will have a mass variation depending on the geometrical parameter, this specific method appears not to be suitable from the beginning. Nevertheless, it is necessary to remind that the real comparison between the different approaches has to be performed on a reduced order model characterized by the application of the Craig-Bampton component mode synthesis: for this reason, the outcomes just illustrated have to be interpreted cautiously.

3.1.2 Reduced order model

After having tested the various methods on a full one-dimensional model, the next step consists in their application on a 1D reduced order model. For this purpose the previous model (see figure 3.1) has been replicated with an higher number of masses and springs (200) and the reduction has been performed through the following passages, repeated for all the five stations: 20 boundary degrees of freedom have been selected in a random way, with the only expedient of not repeating the same dof twice; within the remaining 180 internal degrees of freedom only 30 have been used as slave degrees of freedom. This choice is clearly connected to the degree of approximation that is requested trough the reduction: if all the internal degrees of freedom are conserved, no reduction is performed, while, decreasing gradually their number, the approximation error between the two models grows. Since the treated system is one-dimensional, by considering 20 master degrees of freedom and 30 slaves degrees of freedom the reduced order models will have the mass and stiffness matrices with a 50x50 dimension against a 200x200 dimension for the matrices of the full models. The reduction in this case is not really pronounced, but allows to obtain percentage errors below 1% on the first 20 natural frequencies in the comparison between full and reduced model (for each station) and it is still useful for the application of the different techniques. Additionally, in this case the reference condition has been created trough an analytical full model at the parameter p corresponding to a mass value of 3.08 kg and a stiffness value of $1.578 \cdot 10^6$ N/m. Another important reference is represented by the CB-CMS reduced model at the parameter p of interest: it is a passage that in more complex models won't be executed because it is time-consuming and not explicitly requested (it actually substitutes the role of the interpolation), but at this stage it can give some good indications, especially about the matrices mapping. As usual, the study of the outcomes focuses on the first 10 modes, while the vector of the selected boundary degrees of freedom is reported below together with the natural frequencies of the five stations after the reduction procedure 3.6.

$$b_{vect} = [5, 8, 25, 33, 37, 52, 66, 80, 84, 106, 109, 116, 123, 131, 136, 150, 159, 162, 185, 187]$$

The growing trend of the natural frequencies along the stations is similar to what happened also in the 1D full model; however, the values are generally lower because the reduced order model derives from a system composed by 200 mass and stiffness elements, an higher number compared to the 50 elements of the 1D full model. The theoretical explanation consists in the fact that a model with an high number of degrees of freedom is less rigid (or more deformable) with respect to a model characterized by a low number of degrees of freedom. In general, this is also the reason why a discrete system, as a FEM model, is always stiffer than a continuous system, which tends to the real behaviour.

Mode	freq S1 [Hz]	freq S2 [Hz]	freq S3 [Hz]	freq S4 [Hz]	freq S5 [Hz]
1	0.79	0.82	0.87	0.93	1.01
2	2.38	2.45	2.60	2.80	3.04
3	3.96	4.08	4.33	4.67	5.07
4	5.55	5.71	6.07	6.54	7.10
5	7.13	7.34	7.80	8.42	9.13
6	8.71	8.98	9.53	10.28	11.15
7	10.30	10.61	11.26	12.15	13.18
8	11.88	12.24	12.99	14.02	15.20
9	13.46	13.87	14.73	15.89	17.23
10	15.04	15.49	16.45	17.75	19.25

Table 3.6: Natural frequencies at the 5 stations, 1D ROM model

Taylor series finite differences method

The results obtained through the first interpolation technique in terms of natural frequencies estimation are listed in the table below.

Mode	PROM frequency [Hz]	Test frequency [Hz]	Percentage error [%]
1	0.90	0.89	1.12
2	2.70	2.68	0.75
3	4.51	4.46	1.12
4	6.39	6.25	2.24
5	8.19	8.03	1.99
6	10.28	9.81	4.79
7	12.11	11.60	4.40
8	14.45	13.38	8.00
9	15.87	15.16	4.68
10	16.47	16.94	-2.77

Table 3.7: Natural frequencies comparison, 1D reduced order model, Taylor series interpolation with finite differences (Epureanu et al.[1]) VS analytical model

It can be noticed immediately that the percentage errors are not negligible and also that they do not show a monotonic trend: it is a clear sign about the problems that the Taylor series approximation gives with respect to this type of reduced order model. The situation is even more evident in the MAC representation (figure 3.10 , where, apart from the first few modes, the approximation is quite rough.

By looking into detail at the single modeshapes,if we consider the 3rd mode the interpolation follows the analytical model, while for the 10th mode the overlapping is not reached (figures 3.11 and 3.12).
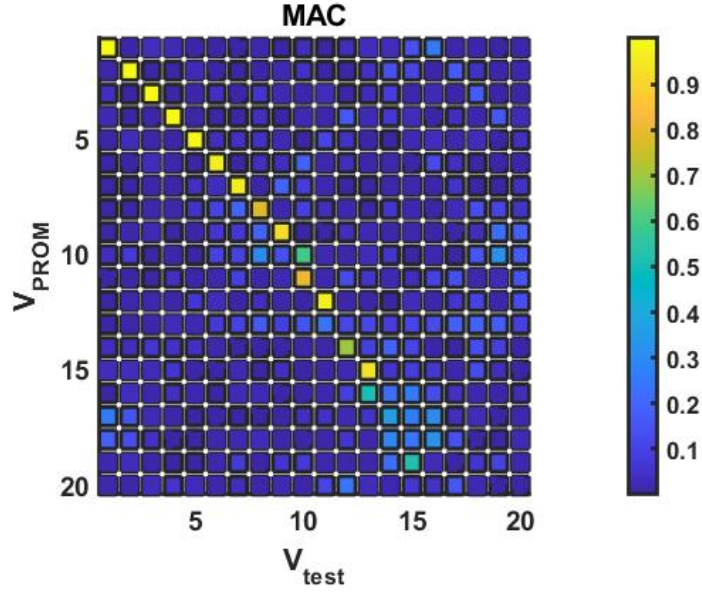
Figure 3.10: MAC, 1D reduced order model, Taylor series interpolation with finite differences (Epureanu et al.[1]) VS analytical model, 20 modes
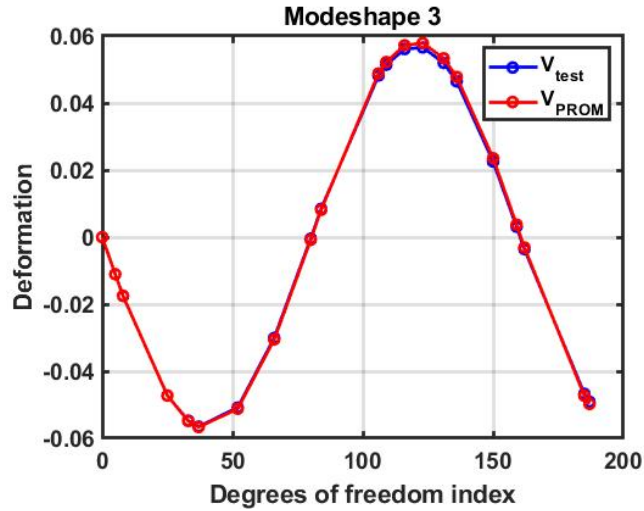
Figure 3.11: Modeshape 3, 1D reduced order model, Taylor series interpolation with finite differences (Epureanu et al.[1]) VS analytical model

The same considerations can be done also in terms of forced response. It is important to underline the fact that in this reduced order model the force was applied with an intensity of 1 N at the 8th master degree of freedom, which corresponds to the 80th global degree of freedom, while the displacement has been detected at the 13th master degree of freedom, correspondent to the 123th global degree of freedom. The choice of applying the force to a master degree of freedom is coherent with re-

Figure 3.12: Modeshape 10, 1D reduced order model, Taylor series interpolation with finite differences (Epureanu et al.[1]) VS analytical model

spect to what it is typically done in this type of models, whereas the displacement amplitude detection can be carried out even considering slave degrees of freedom. If the stimulated mode is one of the first, for example mode 1, characterized by better approximations regarding natural frequencies and eigenvectors, then also in the forced response computed by means of the mode superposition the overlapping (neglecting the small natural frequency discrepancy) will be guaranteed, as represented in figure 3.13.
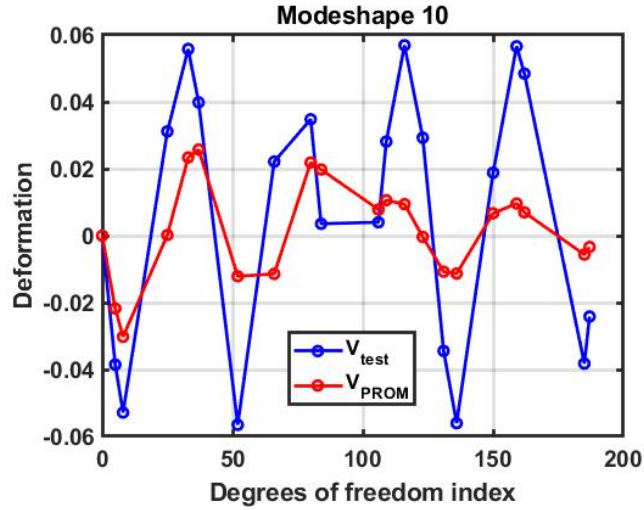

Figure 3.13: Forced response, mode 1, 1D reduced order model, Taylor series interpolation with finite differences (Epureanu et al.[1]) VS analytical model

25

However, if we extend the frequency range in order to include the first 10 modes and then we apply the mode superposition with $N = 10$, we can notice that the curve of the parametric reduced order model traces the reference curve only for the first modes and then diverges from it.
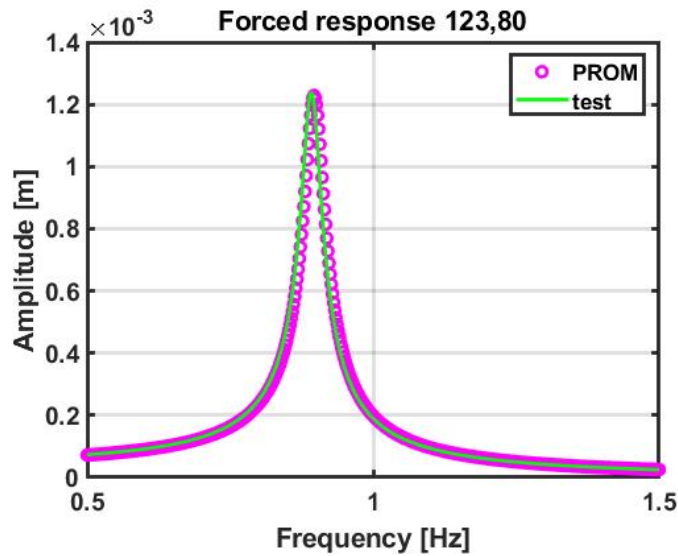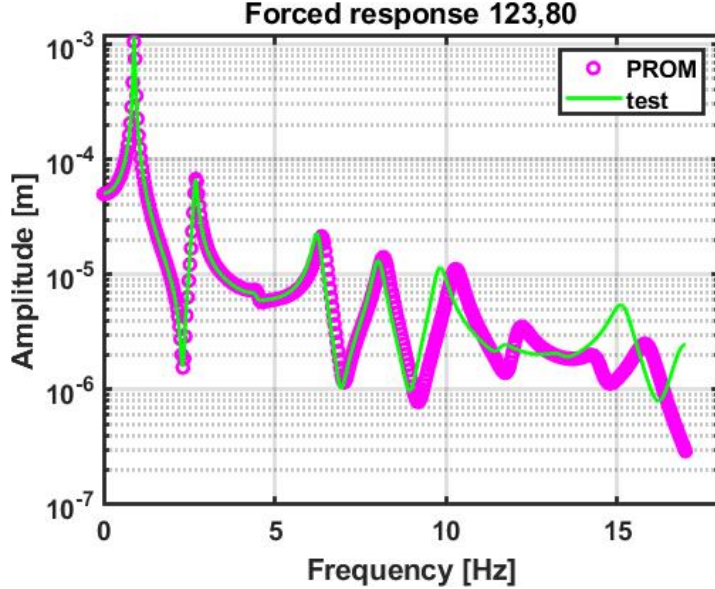

Figure 3.14: Forced response, 1D reduced order model, Taylor series interpolation with finite differences (Epureanu et al.[1]) VS analytical model

For what concerns the matrix conformation, the figures 3.15 and 3.16 illustrate the situation: inside them we find the comparison between the mass and stiffness matrices of the reduced order reference model, that represent the expected result in terms of matrix mapping, and the mass and stiffness matrices of the interpolated system. The figures were obtained trough the Matlab command *spy*.

From this figures it can be noticed that the interpolation does not affect the mapping of the stiffness matrix, which presents a tridiagonal block corresponding to the master-master region and a diagonal block at the slave-slave region. On the other hand, the mass matrix obtained with the parametric reduction technique does not have the exactly same mapping as the reference mass matrix: this aspect is explained by the comparison of nonzero elements for the two matrices and will be more relevant in the 3D models of the next sections.
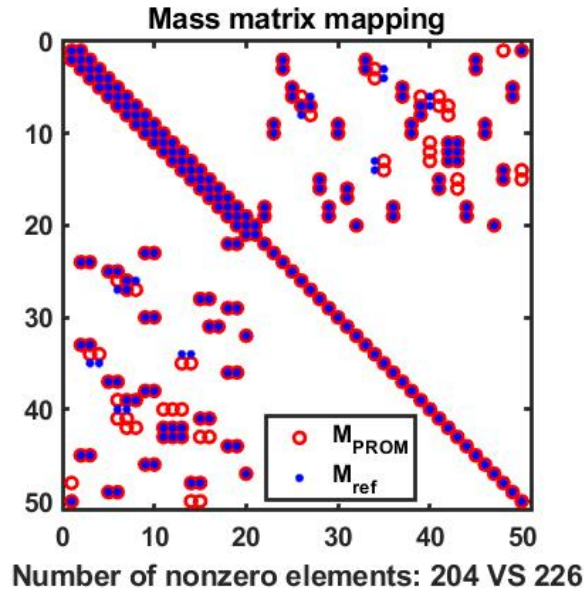
Figure 3.15: Mass matrices, 1D reduced order model, Reference ROM VS Taylor series interpolation with finite differences (Epureanu et al.[1])
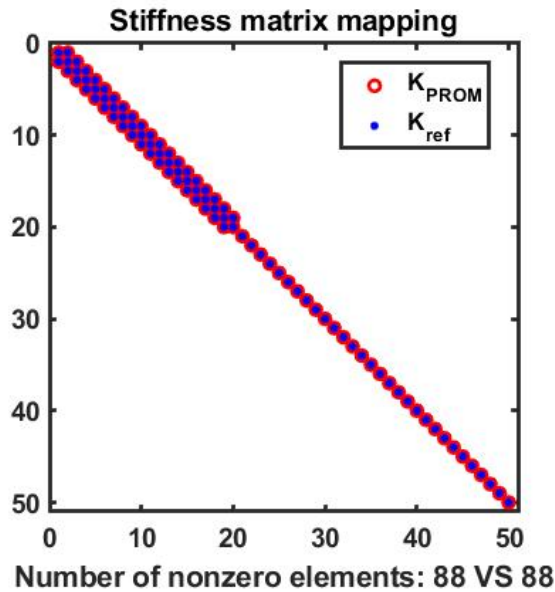
Figure 3.16: Stiffness matrices, 1D reduced order model, Reference ROM VS Taylor series interpolation with finite differences (Epureanu et al.[1])

Element by element interpolation

The second interpolation technique manifests a peculiar problem: the interpolated mass matrix is symmetric but not positive definite, leading to the occurrence of complex modes after the eigenvalue-problem. Whens this happens, it has no meaning

27

to perform the comparison in terms of natural frequencies, modeshapes and forced response. Nevertheless, for the sake of completeness, the MAC diagram and the forced response computed by means of the superposition of 10 modes are reported.
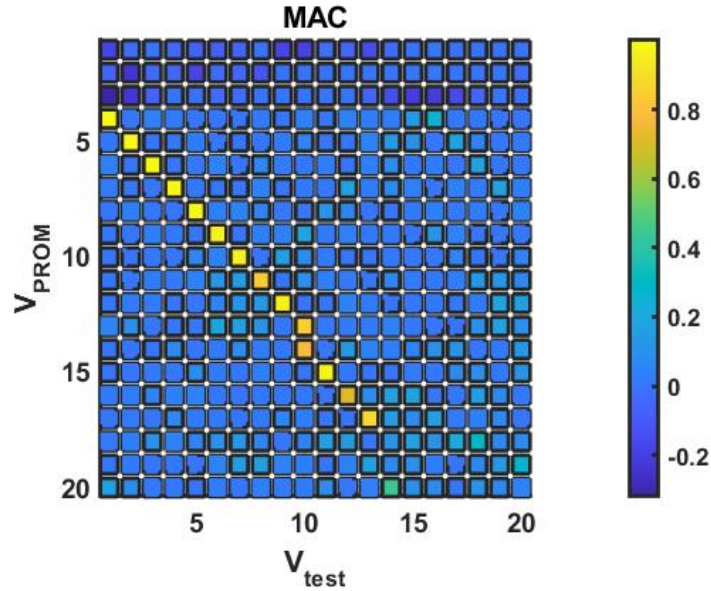
Figure 3.17: MAC, 1D reduced order model, Element by element interpolation VS analytical model, 20 modes
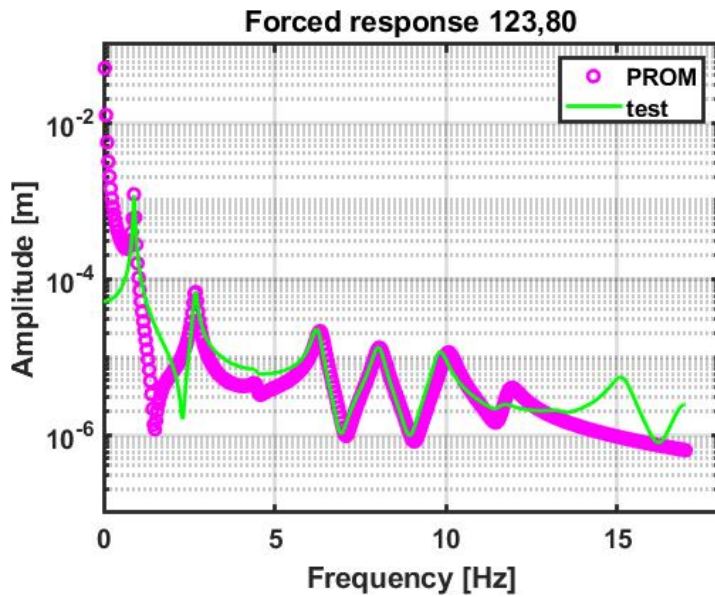
Figure 3.18: Forced response, 1D reduced order model, Element by element interpolation VS analytical model

From these images it is possible to understand that the element by element interpolation method is not completely affected by the presence of complex modes: in fact, in the MAC diagram a correlation between the interpolated eigenvectors and the reference eigenvectors is present, but shifted with respect to the main diagonal; this behaviour appears also in the forced response graph, where the curve of the interpolated model does not match accurately the reference peaks for the first modes, but then follows them with a good approximation. In regard to the matrix mapping, the results are similar to the ones presented in the previous paragraph, with the only difference represented by the parametric reduced order model mass matrix, that shows an higher number of nonzero elements with respect to the reference (figure 3.19): this outcome indicates that the CB-CMS mass matrices of the five stations, from which the interpolation originates, have a different mapping even with the same number of nonzero elements.
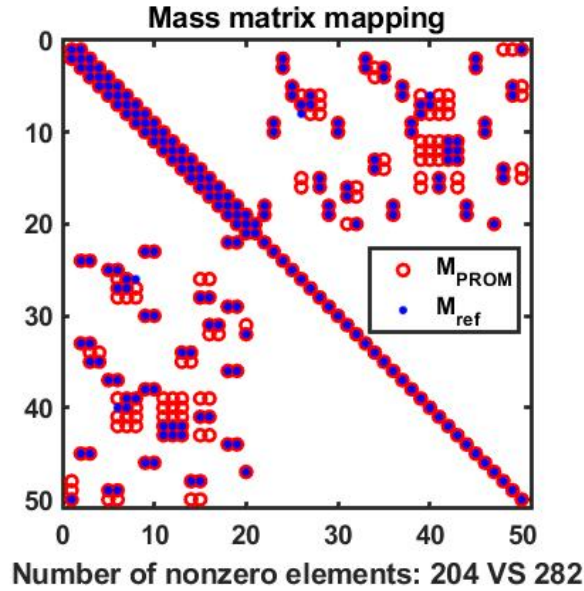
Figure 3.19: Mass matrices, 1D reduced order model, Reference ROM VS Element by element interpolation

Interpolation of eigenvalues and eigenvectors

The natural frequencies computed through the interpolation of the eigenvalues and eigenvectors of the 5 stations and rounded at the second decimal digit are listed in the table 3.8.

From the analysis of the table, this technique is the best for what concerns the natural frequencies estimation, with a maximum error much lower than 1 % within the first 10 modes. Also the MAC computation manifests an accurate matching between the model and the reference, not only for the first modes, as was happening with the Taylor series interpolation, but also for higher index modes.

Mode	PROM frequency [Hz]	Test frequency [Hz]	Percentage error [%]
1	0.89	0.89	0.00
2	2.68	2.68	0.01
3	4.46	4.46	0.01
4	6.25	6.25	0.03
5	8.03	8.03	0.04
6	9.82	9.81	0.04
7	11.61	11.60	0.08
8	13.39	13.38	0.08
9	15.19	15.16	0.18
10	16.97	16.94	0.17

Table 3.8: Natural frequencies comparison, 1D reduced order model, Eigenvalues and eigenvectors interpolation VS analytical model
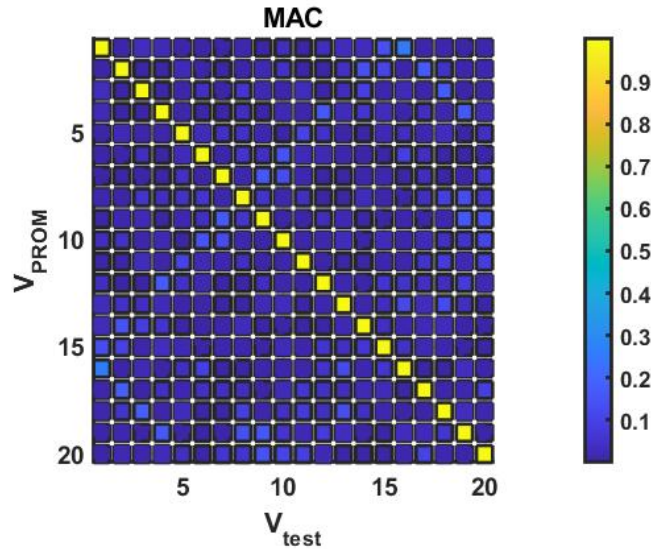
Figure 3.20: MAC, 1D reduced order model, Eigenvalues and eigenvectors interpolation VS analytical model, 20 modes

The positive outcomes are associated to the computation of the forced response too, as demonstrated from figure 3.21.

In relation to the matrices' conformation, the results are reported into figures 3.22 and 3.23: differently from the previous cases, even the interpolated stiffness matrix shows a different mapping compared to the reference one. In particular, the dissimilarities concentrate around the main diagonal in the slave-slave dof portion. In general we can state that the tendency of the parametric reduced order model is to fill more boxes than expected into the matrices $[K_{PROM}]$ and $[M_{PROM}]$.
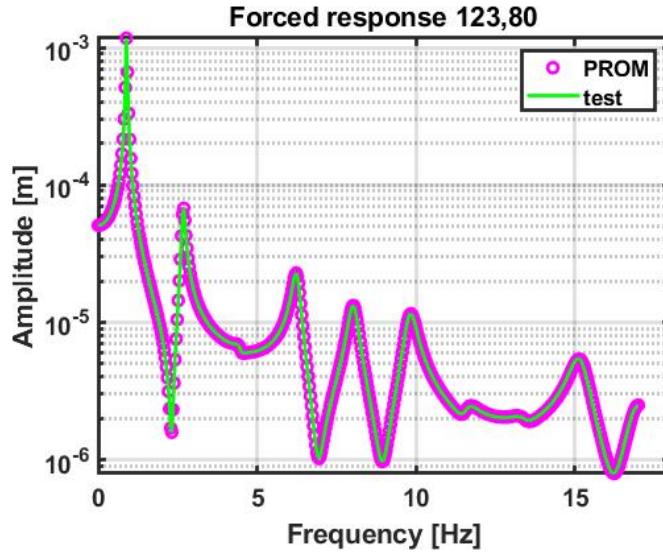
Figure 3.21: MAC and forced response, 1D reduced order model, Eigenvalues and eigenvectors interpolation VS analytical model
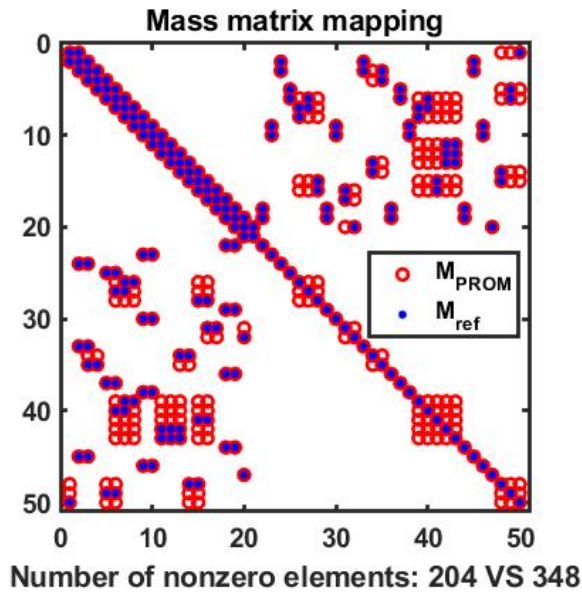
Figure 3.22: Mass matrices, 1D reduced order model, Reference ROM VS Eigenvalues and eigenvectors interpolation

In conclusion, summarizing the main outcomes of the three parametric interpolation techniques applied to a simple one-dimensional reduced order model, it has been demonstrated that the interpolation of eigenvalues and eigenvectors delivers the best results, with the only drawback represented by the variability of the matrices' mapping. The element by element interpolation manifested concrete problems since

31
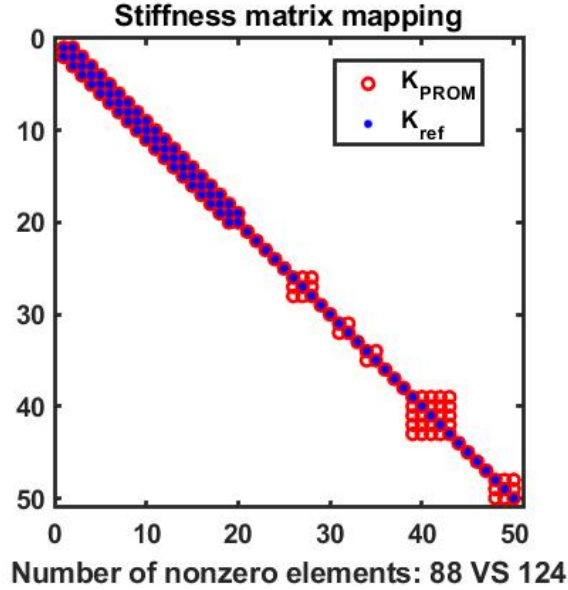
Figure 3.23: Stiffness matrices, 1D reduced order model, Reference ROM VS Eigenvalues and eigenvectors interpolation

it produced unwanted complex modes, while the Taylor series approximation led to higher errors in terms of natural frequencies and MAC. It is important to underline that these results have been obtained with a specific selection of the boundary degrees of freedom employed in the reduction: with a different set of master dof the main differences occurs in the matrix mapping, whereas the other verification are less affected. Another important topic to remark is that the MAC computation has been performed for all the methods by means of the only master degrees of freedom, avoiding to insert in the calculation the slaves degrees of freedom of the eigenvectors. In the same way the forced response computation has been realized by applying the force to a master degree of freedom and detecting the amplitude of displacement at another master degree of freedom. This procedure has been followed even in the more complex models presented in the next sections.

3.2 Cantilever beam
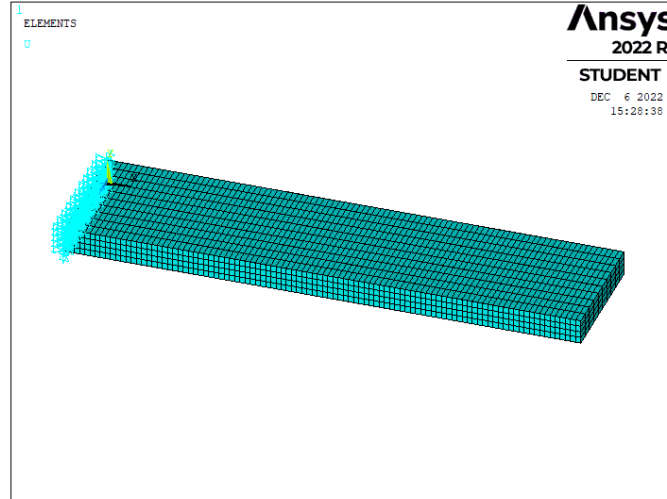
Figure 3.24: Cantilever beam FEM model, Ansys APDL

The second model discussed is a three-dimensional system created by means of the FEM software Ansys Mechanical APDL. It consists in a cantilever beam, with length equal to 200 mm, width equal to 50 mm and a variable thickness. The choice of this kind of system was not random, but in a path of continuity between the previous one-dimensional model and the dummy blade displayed in the next section. In detail, the thickness p plays the role of the perturbed parameter, into an interval of interest around the nominal value (10 mm) defined in table 3.9: as it is possible to observe, two types of pattern have been prepared, the first associated to a tighter selection of the equally spaced stations, the second to a wider selection of them.

| Station N°	1	2	3	4	5
p1 [mm]	9.6	9.8	10	10.2	10.4
p2 [mm]	9.2	9.6	10	10.4	10.8

Table 3.9: Thickness p variation along the 5 stations, tight pattern (1st row), wide pattern (2nd row)

In addition, the material has been assumed to be steel, characterized by the following properties:

- Density $\rho = 7800$ kg/m^3

- Elastic modulus $E = 210$ GPa

- Poisson ratio $\nu = 0.3$

For what concerns the implementation into Ansys, the model has been meshed with 4000 elements and 5555 nodes: in particular the element's type used has been SOLID185, that distinguish itself for being composed by 8 nodes, each one having three translation degrees of freedom; moreover, the element SOLID185 allows for prism, tetrahedral and pyramid degeneration when employed in irregular regions (not necessary in this case). In order to perform the reduction, 16 master nodes, depicted in purple in figure 3.25, have been selected (each of them associated to 3 degrees of freedom) and 100 slaves degrees of freedom were conserved: as a result, the Craig-Bampton CMS reduction technique has allowed to pass from a system of 16665 dof to a system of 148 dof, with negligible percentage errors on the first 20 modes comparison. The selection of the master nodes does not follow any particular pattern but, for convenience, is has been performed in a symmetrical way over the external nodes of the system. The most important aspect is to avoid the selection of the constrained nodes, that cannot show any displacement, but also of the so called "modal nodes", which are point of the structure that does not manifest any relative displacement in some eigenvectors simulation and for this reason can provoke misleading deductions.
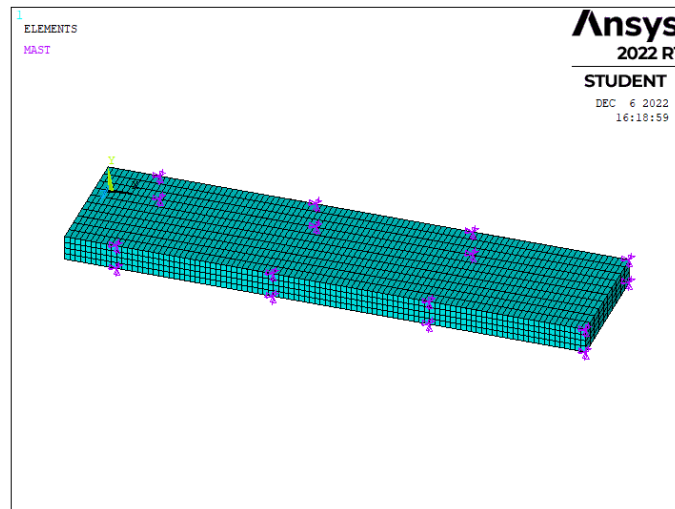
Figure 3.25: Master nodes along the cantilever beam

The whole reduction procedure has been carried out in Ansys, while the matrices extraction and all the other comparisons and verification have been realized into the Matlab environment. For these analyses the reference is represented by a full Ansys model of the cantilever beam, characterized by a value of thickness that does not correspond to one of the 5 stations: for sake of completeness two different reference thicknesses have been individuated, the first (9.7 mm) lower than the nominal value, the second (9.7 mm) higher. Besides, differently from what was done in the one-dimensional model, the analysis focuses on the first 20 modes of the structure, both in terms of natural frequency estimation, MAC and forced response computation.

3.2.1 Taylor series finite differences method

We start our study considering the interpolation technique based on the Taylor series approximation, with the derivatives written through finite differences terms. The selected pattern of the five stations is the first, with a distance Δp between two consecutive stations equal to 0.2 mm, whereas the reference system is represented by the cantilever beam model with thickness 9.7 mm. Similarly to what happened in some cases during the examination of the one-dimensional reduced order model, the results are affected by the fact that the interpolated matrix is not positive definite: this leads to the occurrence of complex eigenvectors associated to negative eigenvalues that do not enable to perform the complete analysis. In detail, since the modes are listed along the column of the modal matrix by growing real part of the eigenvalues, the complex eigenvectors take position in the first columns, associated to eigenvalues with null real part. After this columns' series occupied by the complex eigenvectors, the real eigenvectors are listed. The situation is well described by the MAC diagram, where it is possible to notice a correlation between the interpolated modes and the reference modes starting from the 18th mode of the PROM (red circled region).
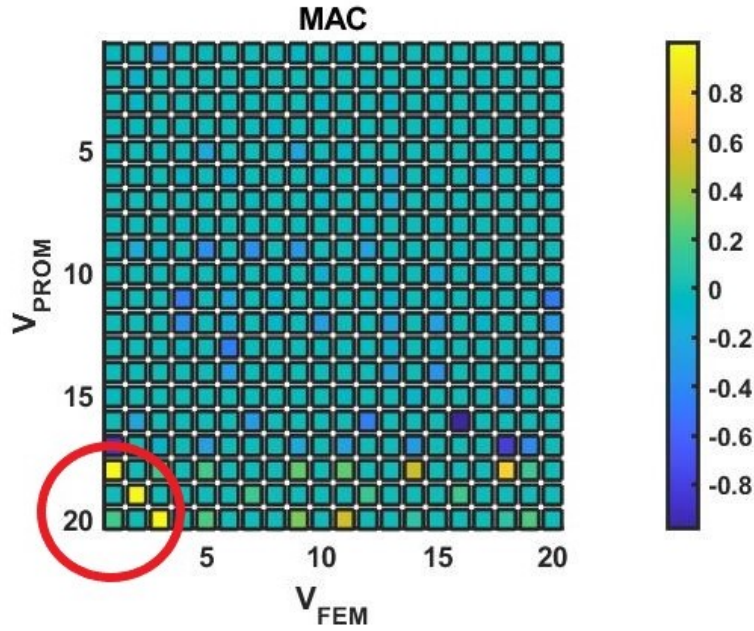
Figure 3.26: MAC, Cantilever Beam, Taylor series interpolation with finite differences (Epureanu et al.[1]) VS Full reference model, 9.7 mm, 20 modes

In terms of eigenvalues, the phenomenon is even more clear: in table 3.10 are reported the natural frequencies of the model at the interpolated condition, against the FEM reference model's natural frequencies: the first start from a mode index equal to 18 (it means that 17 complex modes are present), while the second start from a mode index equal to 1.

| Mode	PROM frequency [Hz]	FEM frequency [Hz]	Percentage error [%]
1	205.5	205.4	0.05
2	1004.2	1004.2	0.00
3	1273.5	1273.2	0.02
4	1534.4	1533.7	0.04
5	3513.0	3513.1	-0.00
6	4701.5	4701.8	-0.01
7	5103.2	5103.7	-0.01
8	6510.3	6510.5	-0.00
9	6745.1	6745.7	-0.01
10	8148.7	8149.3	-0.01
11	10860	10869	-0.08
12	11699	11733	-0.29
13	11999	12007	-0.00
14	15605	15748	-0.91
15	16343	16356	-0.08
16	17238	18960	-9.08
17	17984	19436	-7.47
18	19435	20133	-3.47
19	19906	21222	-6.20
20	21211	21229	-0.08

Table 3.10: Natural frequencies comparison, Cantilever Beam, Taylor series interpolation with finite differences (Epureanu et al.[1]) VS Full reference model, 9.7 mm

By observing the data stored in the table it seems that the technique could work effectively, at least for the some modes. However, it is not possible to predict in advance how many complex modes will appear after the interpolation and this could represent a big limitation inside the procedure. It is also useful to see what happens if we perform the analysis considering as a reference another value of thickness, for example $p = 10.1$ mm. It is a condition which is closer to the nominal thickness (10 mm) and it gives better results with respect to the previous, as described by the MAC diagram depicted in figure 3.27. By observing the figure it is easy to understand that the MAC manifests values close to 1 along the main diagonal until the 10th mode, but from then on the correlation shifts along the first inferior off-diagonal, as if a spurious mode was created in the interpolated model (row 11). Even if the match in terms of modeshapes is not perfect, it is important to underline that it has not been generated any complex eigenvector. For sake of completeness, the natural frequencies comparison table and the forced response graph are reported too.
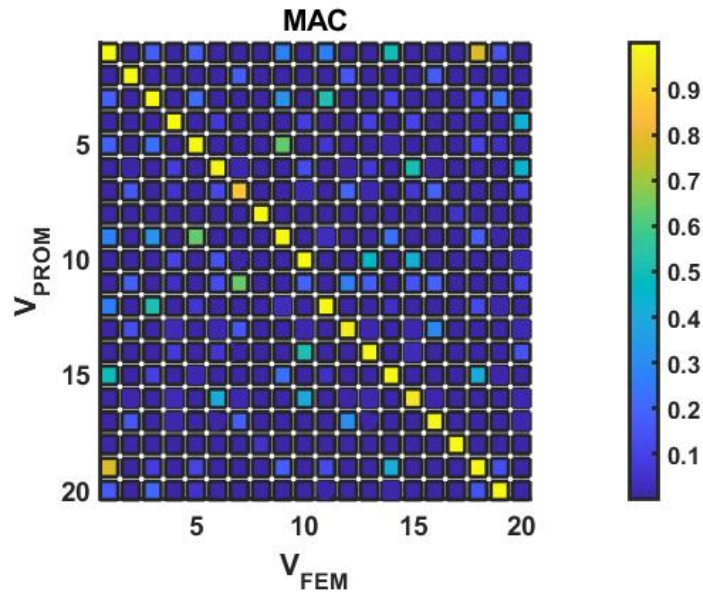
Figure 3.27: MAC, Cantilever Beam, Taylor series interpolation with finite differences (Epureanu et al.[1]) VS Full reference model, 10.1 mm, 20 modes

Looking at table 3.11 the problematic described in the MAC analysis becomes even more clear: the percentage errors are quite low (apart from mode 7) until the 10th mode, then they tend to grow, with the maximum absolute value given by almost 20%. However, it is also possible to notice a correlation between the 12th mode obtained with the PROM and the 11th reference mode, as well as between the 13th PROM mode and the 12th reference mode and so on: it is the effect of the presence of a spurious mode already identified into the MAC diagram. In addition, if we make a comparison between the reference natural frequencies, we can individuate a group of modes that do not vary a lot their eigenvalues along the thickness increment (modes 2,7,8,12,16,17). By plotting their modeshapes into Ansys APDL we can recognize that they are bending modes in the X-Z plane, which is perpendicular to the stiffness direction, or axial modes.
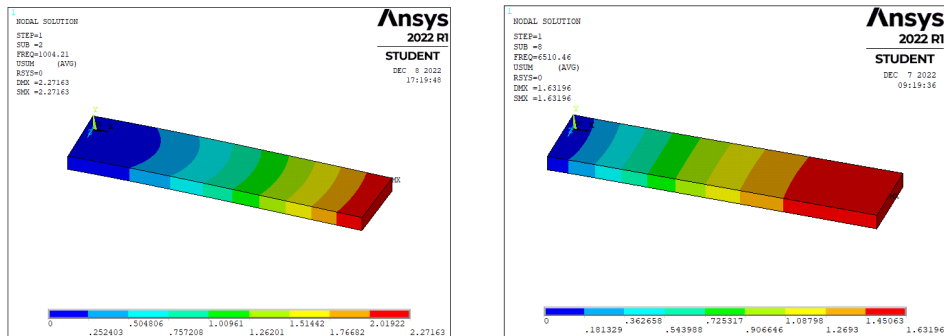
Figure 3.28: Modeshapes 2 and 8, Cantilever beam, Full reference model, 9.7 mm

Mode	PROM frequency [Hz]	FEM frequency [Hz]	Percentage error [%]
1	213.8	213.7	0.05
2	1004.3	1004.3	0.00
3	1323.5	1323.2	0.02
4	1596.1	1588.7	0.47
5	3646.9	3646.4	0.01
6	4884.4	4867.7	0.34
7	5436.5	5103.9	6.52
8	6510.8	6510.7	0.00
9	6989.5	6849.4	-0.01
10	8494.5	8428.4	2.04
11	10628	11240	-5.44
12	11242	11733	-4.18
13	11789	12402	-4.94
14	13105	16250	-19.35
15	16256	16868	-3.63
16	17083	18960	-9.90
17	18977	19436	-2.36
18	20155	20720	-3.47
19	20732	21844	-2.73
20	21866	21856	0.05

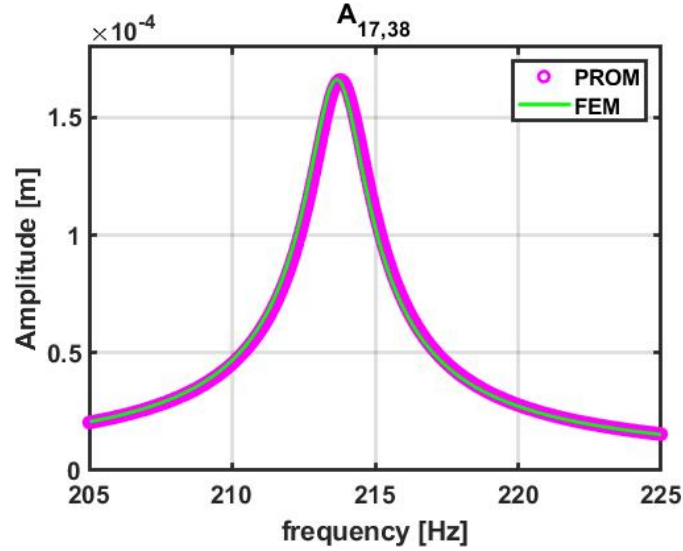**Table 3.11:** Natural frequencies comparison, Cantilever Beam, Taylor series interpolation with finite differences (Epureanu et al.[1]) VS Full reference model, 10.1 mm

The forced response comparison is carried out by applying a force of intensity 1 N to the 38th master degree of freedom, which corresponds to the Y-dof of the master node 607, while the displacement detection takes place on the 17th master degree of freedom, namely the Y-dof of the master node 136. The damping factor ζ is assumed to be equal to 0.005 for both models, while the frequency vector has been subdivided into 1000 intervals. The procedure adopted to perform the computation is the mode superposition, including the first 5 modes: this choice clearly limits the frequency range selected for the comparison, but since we're interested into the 1st mode solicitation, it is surely an acceptable decision.

The figure 3.29 demonstrates that the outcomes are positive, since the match between the two models is almost perfectly reached. This testify also that the Taylor series interpolation with the derivatives approximated by means of finite differences terms can give quite good result when the analysis is performed really close to the nominal value of the perturbed parameter (10 mm in this case), and in general when the perturbation does not influence the positive definite matrices, whereas it introduces many problems (complex eigenvalues) in all the other conditions.

Figure 3.29: Forced response, Cantilever beam, Taylor series interpolation with finite differences (Epureanu et al.[1]) VS Full reference model, 10.1 mm

3.2.2 Element by element interpolation

For what concerns this method, the outcomes and deductions are almost the same as the ones faced into the previous paragraph: independently from the reference and from the width of the stations' pattern, the interpolated mass matrix is symmetric but not positive definite, with the consequent appearance of complex eigenvectors, as demonstrated also by the MAC diagram.
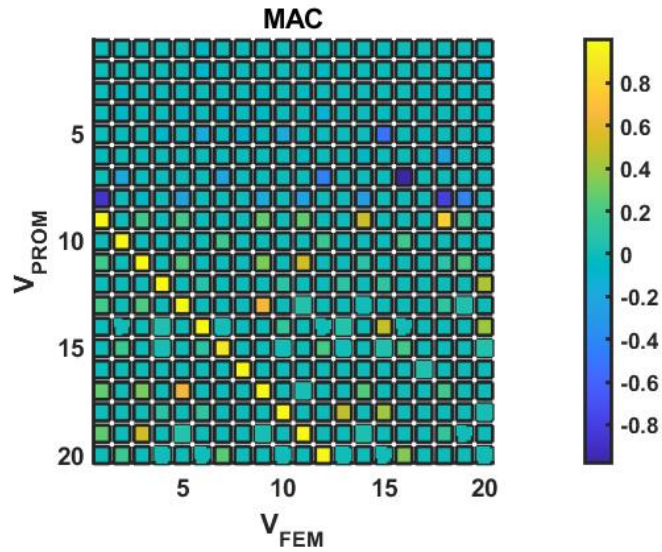
Figure 3.30: MAC, Cantilever Beam, Element by element interpolation VS Full reference model, 9.7 mm, 20 modes

Even here the correlation between interpolated and reference eigenvectors starts with a certain delay with respect to the main diagonal, pointing out the presence of 8 complex modes. In regard to the natural frequencies approximation the results are even worse with respect to the Taylor series interpolation, as the percentage errors reach values over the 20% for the higher modes, even taking into account the shift imposed to the PROM mode indices. In this conditions the computation of the forced response loses its meaning, whereas the only positive aspect is represented by the conservation of the matrices conformation or mapping, typical of a CB-CMS reduced order model, as illustrated in the next figures.
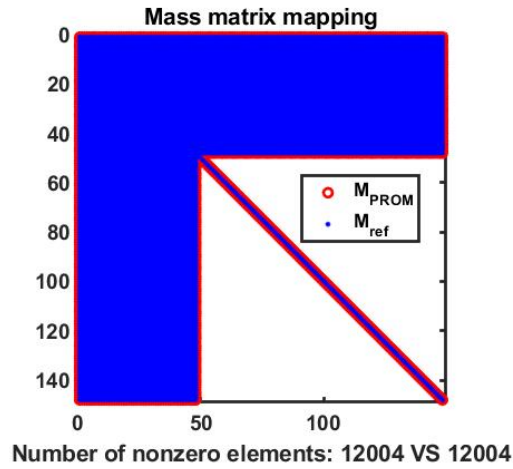
Figure 3.31: Mass matrices, Cantilever beam, Nominal ROM VS Element by element interpolation
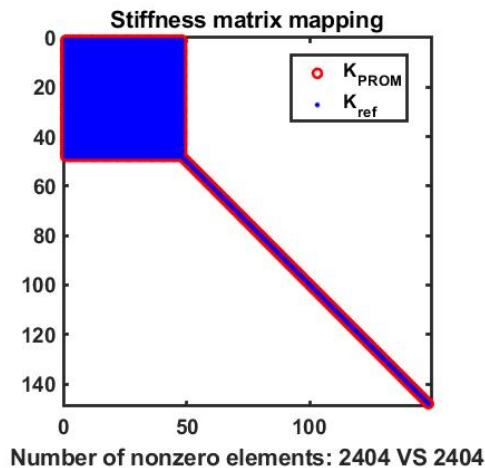
Figure 3.32: Stiffness matrices, Cantilever beam, Nominal ROM VS Element by element interpolation

Additionally, these outcomes are not affected by the choice of the full reference

model: it means that complex eigenvectors can arise for all the perturbed values of thickness p.

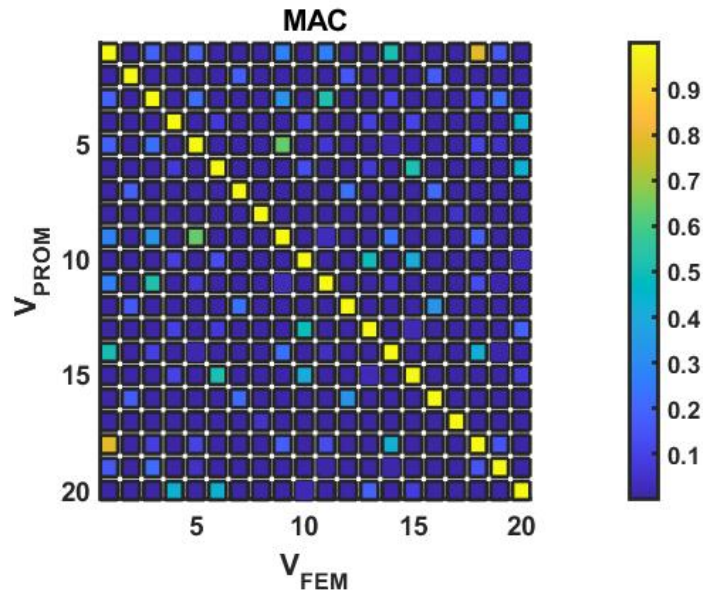### 3.2.3   Interpolation of eigenvalues and eigenvectors

The third technique is the one that provides the best results, both in terms of natural frequencies, MAC and forced response. Starting from the natural frequencies estimation, the table 3.12 reports the results of the interpolated system with a thickness equal to 9.7 mm and compares them to the outcomes of the full reference model.

Mode	PROM frequency [Hz]	FEM frequency [Hz]	Percentage error [%]
1	205.4	205.4	0.00
2	1004.2	1004.2	0.00
3	1273.2	1273.2	0.00
4	1533.8	1533.7	0.00
5	3513.2	3513.1	0.00
6	4701.9	4701.8	0.00
7	5103.7	5103.7	0.00
8	6510.5	6510.5	0.00
9	6745.9	6745.7	0.00
10	8149.5	8149.3	0.00
11	10870	10869	0.01
12	11733	11733	0.00
13	12007	12007	0.00
14	15748	15748	0.00
15	16357	16356	0.01
16	18960	18960	0.00
17	19436	19436	0.00
18	20134	20133	0.01
19	21224	21222	0.01
20	21230	21229	0.00

Table 3.12: Natural frequencies comparison, Cantilever Beam, Eigenvalues and eigenvectors interpolation VS Full reference model, 9.7 mm

It can be noticed immediately that the interpolated natural frequencies match almost perfectly the reference results, which come from a modal analysis performed on the full model into Ansys APDL. The effectiveness of the method is clear also from the observation of the MAC diagram (figure 3.33), where values close to 1 are reached along the main diagonal: in all the other areas of the matrix the correlation between eigenvectors is lower, but in some positions the MAC assumes higher values, that testify a connection between different modeshapes.

Figure 3.33: MAC, Cantilever Beam, Eigenvalues and eigenvectors interpolation VS Full reference model, 9.7 mm, 20 modes

For example, if we consider the 1st reference mode and the 18th PROM mode, the MAC value at the corresponding cell is equal to 0.787: in order to have a more accurate idea about the reason of this correlation, it is possible to plot both modes in Ansys and compare their modal displacements, reported in figure 3.34. The first mode is completely flexural and the 18th mode has a torsional-flexural behaviour with an apparently dominant bending component: if the PROM replicates appropriately the 18th mode, then the high MAC value finds its reason into the previous explanation.
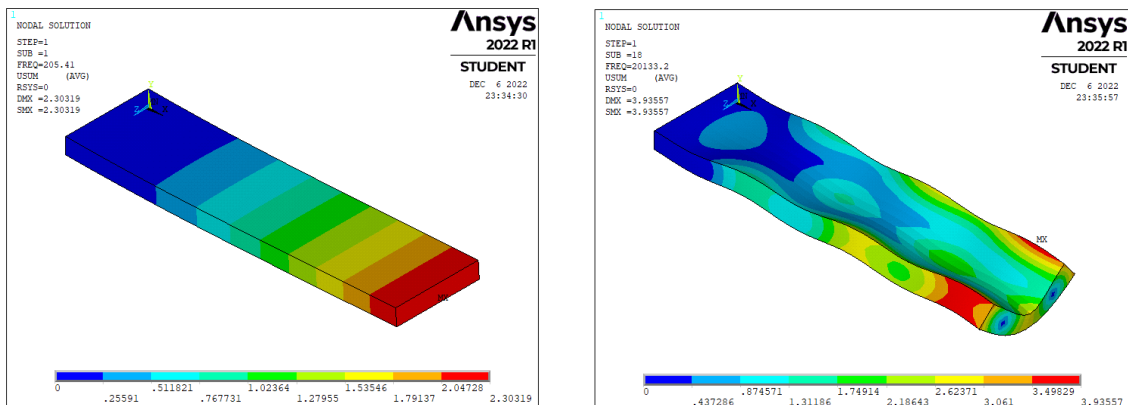
Figure 3.34: Modeshapes 1 and 18, Cantilever Beam, Full reference model, 9.7mm

It is also important to remind that the MAC computation is performed considering only the master degrees of freedom of the reduced order model.
For what concerns the forced response, the assumption were described in the Taylor series paragraph and the results are presented in the figure 3.35, which focuses on the 1st mode solicitation and frequency range.
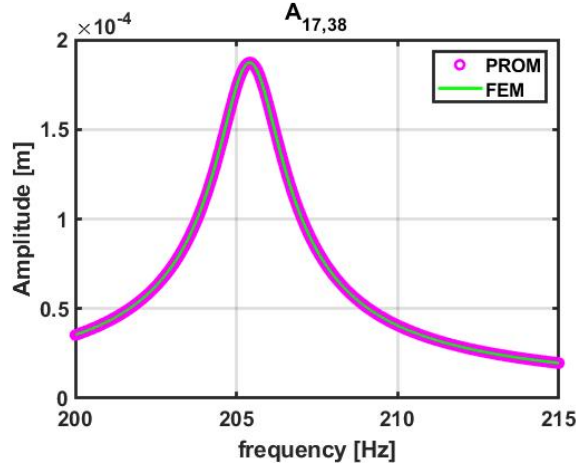
Figure 3.35: Forced response, Cantilever beam, Eigenvalues and eigenvectors interpolation VS Full reference model, 9.7 mm

The figure shows an almost perfect match between the results coming from the two models, a further certification about the goodness of the described method. The main drawback consists in the matrix mapping: while trough the previous techniques the matrix conformation was not perturbed, by means of the interpolation of eigenvalues and eigenvectors the output mass and stiffness matrices $[M_{PROM}]$ and $[K_{PROM}]$ are full. This problem is illustrated in figures 3.36, taking as reference the CB-CMS stiffness matrix of the nominal station.
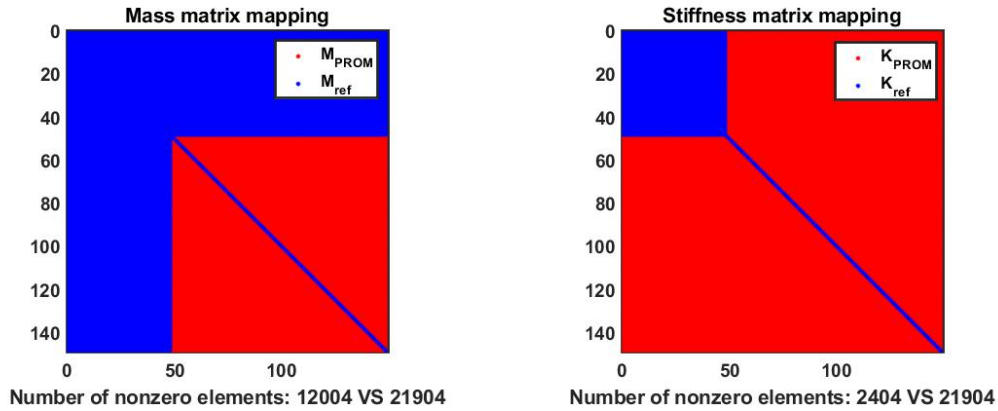

Figure 3.36: Mass and stiffness matrices, Cantilever beam, Nominal ROM VS Eigenvalues and eigenvectors interpolation

Although this outcome is unwanted, it does not create dramatic issues inside the procedure: the main implications are the major difficulty to handle a full matrix with respect to a sparse one and its higher computational cost.

For what concerns the second reference model, created with a value of thickness equal to 10.1 mm, the outcomes and deductions are almost the same. It is more interesting to change the 5 stations pattern, choosing the wider one, characterized by $\Delta p = 0.4$ mm. The main issue that regards this pattern selection, and that was not present with the tight pattern, is dictated by the exchange of some eigenvectors position between consecutive stations. In fact, when the interval between two consecutive stations becomes larger, it is possible that some modes, in particular the ones that show a strong dependence from the thickness variation, change their position inside the modal matrix with the modes that, on the other hand, are less affected by the parameter perturbation. For example this is what happens between the reduced order model stations 1 and 2 and between stations 4 and 5, as represented in the following MAC diagrams (figures 3.37 and 3.38)
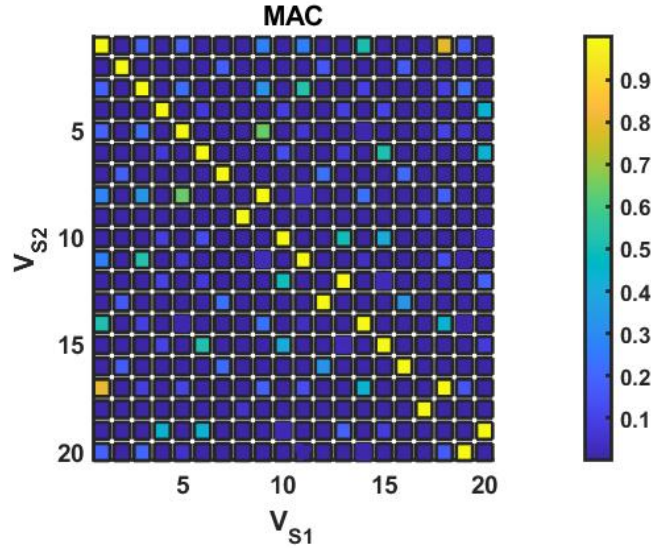
Figure 3.37: MAC, Cantilver Beam, station 1 VS station 2

Considering the first two stations, the exchange of eigenvectors position is indicated by the yellow cells out of the main diagonal: in detail, the 8th mode of station 1 corresponds to the 9th mode of station 2 and vice versa.
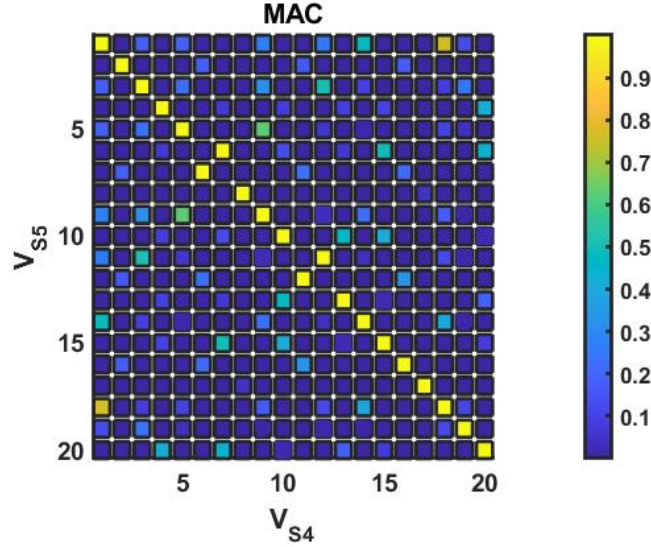
**Figure 3.38:** MAC, Cantilver Beam, station 4 VS station 5

The situation is also visible from the natural frequencies point of view, as illustrated in table 3.13, which lists the first 10 natural frequencies along the 5 station with the wide pattern.

Mode	freq S1 [Hz]	freq S2 [Hz]	freq S3 [Hz]	freq S4 [Hz]	freq S5 [Hz]
1	195.1	203.3	211.6	219.86	228.11
2	1004.1	1004.2	1004.3	1004.3	1004.4
3	1210.5	1260.6	1310.7	1360.6	1410.5
4	1464.0	1519.9	1575.0	1629.5	1683.2
5	3345.3	3479.6	3613.1	3745.8	3877.5
6	4491.0	4659.9	4826.5	4990.6	5104.3
7	5103.4	5103.6	5103.9	5104.1	5152.2
8	6437.1	6510.4	6510.7	6510.9	6511.2
9	6510.2	6684.3	6928.8	7170.4	7409.1
10	7793.6	8078.8	8359.1	8634.6	8905.1

Table 3.13: Natural frequencies at the 5 stations, Cantilever beam, wide pattern $\Delta p = 0.4$ mm

In fact, if we look at the 8th row of the table, we can see a natural frequency value almost constant along all the stations apart from the 1st, which present a lower value. However, we can also notice that the 9th mode of the first station has a natural frequency much closer to the 8th natural frequencies of all the other stations: this means that at the first station the 8th mode, which is of bending type, has a lower natural frequency with respect to the 9th mode, which is of axial type; on the contrary, in the following stations the bending mode has an higher natural frequency with respect to the axial one.
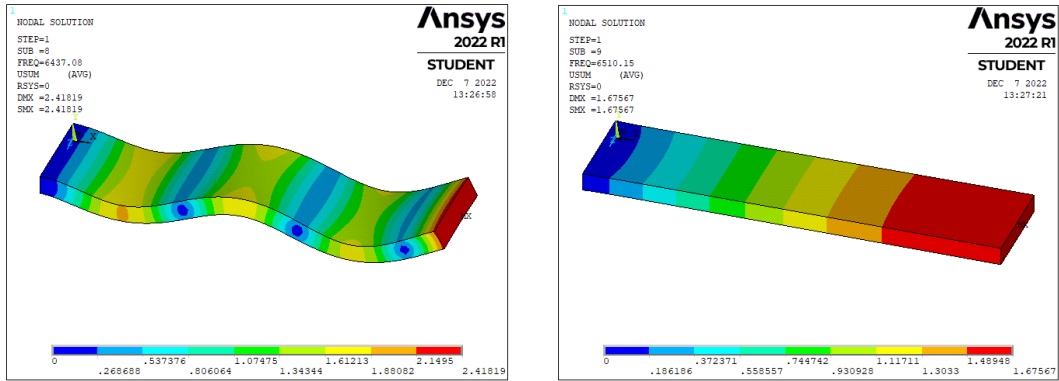
Figure 3.39: Modeshapes 8 and 9, Cantilever Beam, First station, wide pattern $\Delta p = 0.4$ mm

The behaviour just described is only an explanatory example, but in general the tendency is to have more switching modes when the interval between consecutive stations is wider: this situation could represent a problem for the interpolation of eigenvalues and eigenvectors method, leading to distorted results. Therefore, the method must contain a preliminary check, not only on the eigenvectors sign, but also on the MAC computed for each station with respect to the nominal one: if some consecutive modes are switched in comparison with what happens at the nominal station, then they must be rearranged properly. The idea is to have 5 stations characterized by the same eigenvectors sequence before the interpolation. The whole procedure is realized in Matlab, and for the MAC computation takes into account, as usual, only the master degrees of freedom. In the next page are reported the MAC diagrams (figures 3.40 and 3.41) of two different cases: in the first the eigenvectors sorting was not performed, while in the second case the modal and eigenvalues matrices of the five stations were properly rearranged. The reference is represented by a full model created into Ansys APDL, with a thickness value equal to $p = 9.5$ mm, in order to be included between the above-mentioned stations.

The difference between the two graphs is clear and confirms that the eigenvectors rearrangement is useful. In the end it is correct to underline that this further passage has been performed focusing on the switch between consecutive eigenvectors, that in the MAC plot are represented by values close to 1 along the first upper diagonal and first lower diagonal. If the system is much more articulated, the reordering of the eigenvectors could be really difficult to perform and the results after the interpolation would be worse.
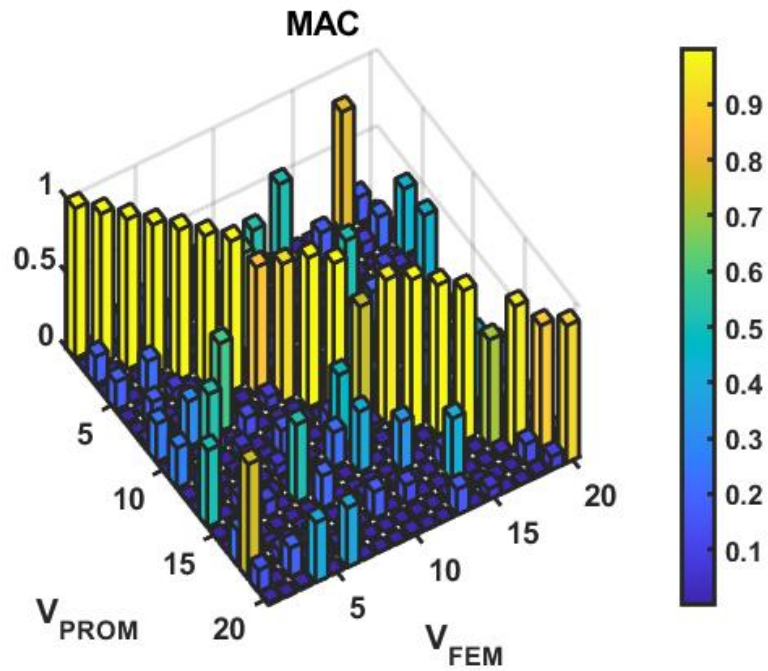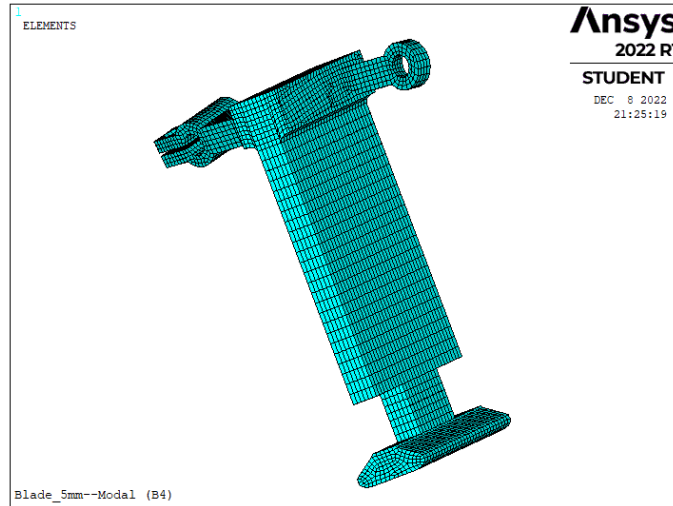
Figure 3.40: MAC, Cantilever Beam, Eigenvalues and Eigenvectors interpolation VS full reference model, 9.5 mm, without eigenvectors sorting
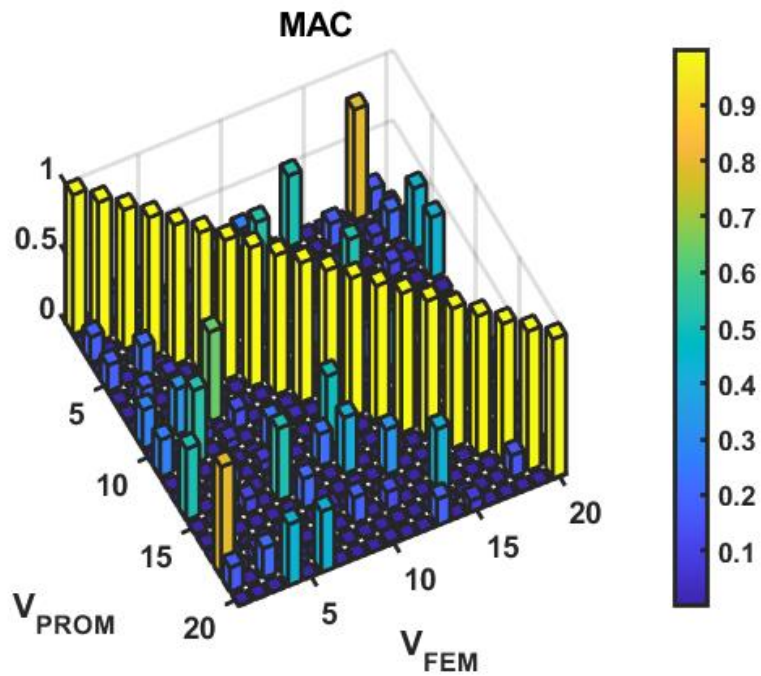
Figure 3.41: MAC, Cantilever Beam, Eigenvalues and Eigenvectors interpolation VS full reference model, 9.5 mm, with eigenvectors sorting

3.3 Blade

**Figure 3.42:** Dummy blade FEM model, Ansys APDL

The third and last model faced consists in a dummy blade, characterized by a simplified geometry with respect to the industrial components. In detail the blade has a main central prismatic body, a rounded inferior part, appositely shaped for the connection with the disk sector, and an upper portion with two particular features that play the role of the shroud, to guarantee the connection also with other blades. Moreover the assigned material, which is steel, has the following properties:

- Density $\rho = 7800$ kg/m^3

- Elastic modulus $E = 206$ GPa

- Poisson ratio $\nu = 0.3$

Before performing the simulation of the various techniques, it has been chosen to constrain the blade at two specific and symmetric surfaces, which in the reality are the contact area between the blade itself and the disk sector. In figure 3.43 it is reported a further zoom over these regions.

For what concerns the application of the various interpolation techniques, it was natural to chose the cross sectional thickness (figure 3.44) of the main body as the parameter p: in this way, the procedure does not deviate consistently from what was done in the cantilever beam model and most importantly, this geometry feature selection surely affects the dynamic behaviour of the blade, as desired. The pattern identification criterion has been motivated even in this case by the percentage variation of the first natural frequency of the extreme station with respect to the nominal one, corresponding to a thickness value of 5 mm: as in the previous section, two different types of pattern have been created, the first tighter and the second wider (table 3.14)
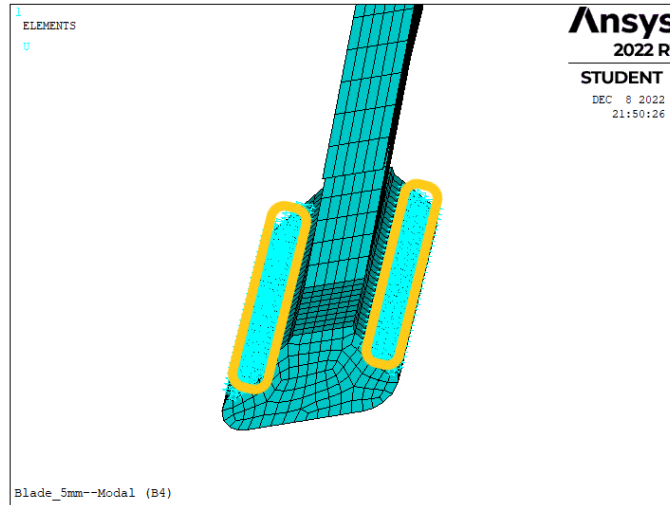
Figure 3.43: Detail about the blade constrained nodes
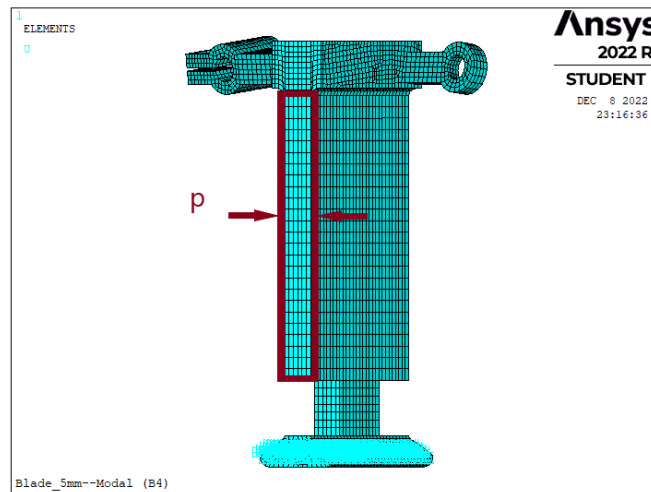
Figure 3.44: Schematic representation of the cross sectional thickness of the blade

Station N°	1	2	3	4	5
p1 [mm]	4.8	4.9	5	5.1	5.2
p2 [mm]	4.6	4.8	5	5.2	5.4

Table 3.14: Thickness p variation along the 5 stations, tight pattern (1st row), wide pattern (2nd row)

Passing to the FEM model description, it is important to explain how this was created. Firstly, the original CAD file of the blade was imported into the software Hypermesh, where the mesh was generated by means of the solid mapping procedure: this technique consists in creating a 2D mesh over some selected faces and then

filling the volumes through a mesh extrusion. At the end of the meshing phase the model was composed by 14606 elements and 69079 nodes, but the most important aspect that Hypermesh allowed was the possibility of modifying the mesh in a really efficient way, in order to create the 5 stations: this particular tool, called "Mesh Morphing", has been inserted separately into the appendix of this thesis, with the aim of writing a step by step tutorial useful also for other research activities. Coming back to our model, the default 3D element type present in Hypermesh is CHEXA8 which corresponds to the element SOLID185 of Ansys; however, for the purpose of performing a more detailed analysis, it was possibile to increase the elements' order and obtain the element type CHEXA20, corresponding to the SOLID186 element of Ansys. This latter is an higher order 3D solid element with 20 nodes, each of them having three translation degrees of freedom.
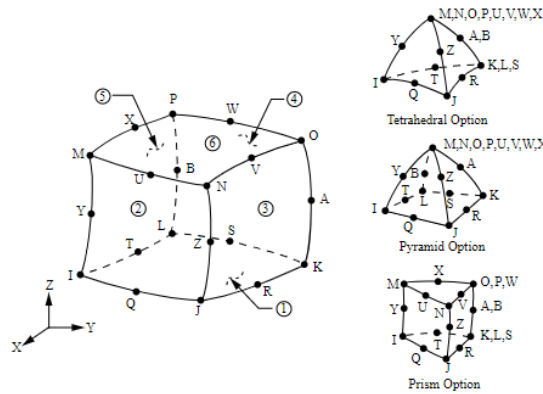

Figure 3.45: SOLID186 element, Ansys APDL

The reduction has been carried out selecting 100 master nodes and as a consequence 300 master degrees of freedom, while the slaves degrees of freedom conserved were 100: this means that the reduced order model for each station had matrices dimensions equal to 400x400. The master nodes have been picked along all the blade, clearly avoiding the nodes already constrained; their number is quite high, but it was a conservative choice, aimed at making sure the effectiveness of the reduction, at least for the first 20 modes. In figure 3.46 are reported in purple the master nodes selected during the Craig-Bampton CMS reduction.

For what concerns the reference model, it has been created a unique FEM full system with a cross-section thickness value equal to 5.14 mm, that has been compared to the interpolated model in terms of natural frequencies, MAC and forced response. Regarding this last topic, the force has been applied with a really high intensity (1000 N) at the 287th master degree of freedom, which corresponds to the Y-dof of the node 16952, while the displacement has been detected on all the master nodes, in particular at the 203th master degree of freedom, corresponding to the Y-dof of the master node number 14859. Finally, the damping factor has been imposed equal to 0.005.
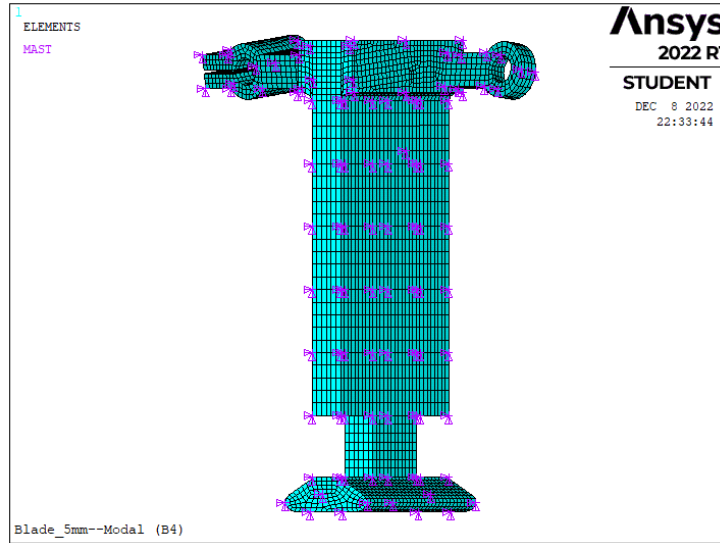
Figure 3.46: Master nodes along the dummy blade

Many of the problems regarding the application of the Taylor series with finite differences method and the element by element interpolation have already been faced in the cantilever beam study and are present also in this model, in an even more pronounced way: both procedures manifest the occurrence of complex modes that do not allow to obtain complete and meaningful results; for this reason in the next paragraph only the interpolation of eigenvalues and eigenvectors technique will be exposed, highlighting advantages and drawbacks.

3.3.1 Interpolation of eigenvalues and eigenvectors

We start our analysis making some considerations about the patterns used and the eigenvectors sorting. At this step the selected pattern is the tighter, which manifests only one exchange of consecutive eigenvectors between stations 3 and 4, as depicted in the MAC figure 3.47.

In particular, it is possible to notice that the 16th eigenvector of station 3 corresponds to the 17th eigenvector of station 4 and vice-versa. If we plot these mode-shapes into Ansys APDL we can recognize a peculiar behaviour, visible in figure 3.48: both are modes that express the higher relative displacement in proximity of the shroud hook; however, while mode 16 is characterized also by a bending component along the main body, mode 17 does not have this behaviour.

Even if our reference model does not fall into the interval between stations 3 and 4, it is important to underline the presence of exchanging modes along the stations also with the tight pattern: this fact corroborate the choice of performing a preliminary eigenvectors sorting taking as a reference the sequence of the nominal station eigenvectors, independently from the amplitude Δp of the pattern used.
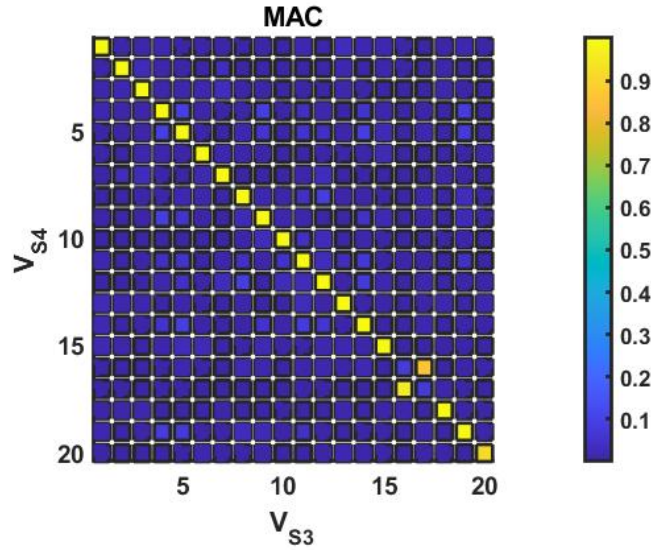
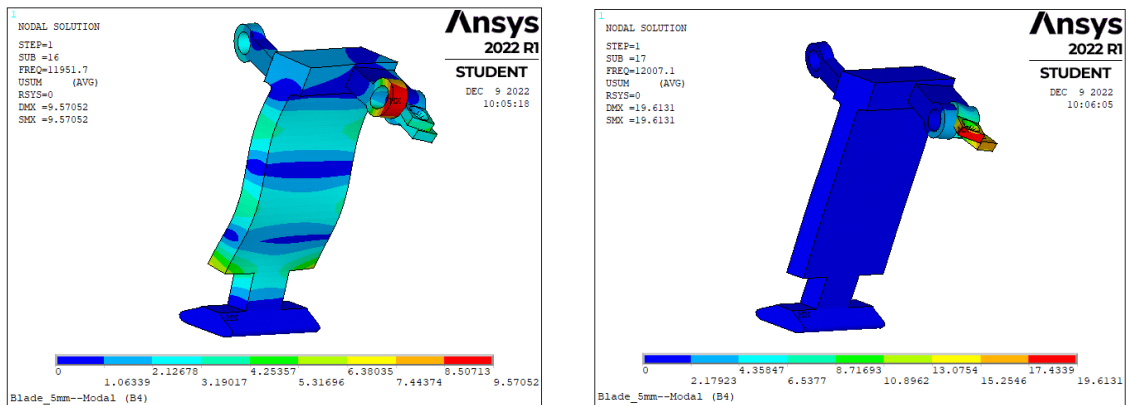**Figure 3.47:** MAC, Blade, station 3 VS station 4, 20 modes

**Figure 3.48:** Modeshapes 16 and 17, Blade full model, station 3

Moving forward, the comparison between the natural frequencies of the interpolated system and the ones of the reference FEM full model, considering the first 20 mode, is performed in table 3.15. It is immediately observable that the percentage errors are almost negligible, a clear sign about the quality of the method. Even the MAC diagram, illustrated into fig 3.49, demonstrates the perfect match between the two models. In addition, differently from what happened in the cantilever beam model, all of the terms out of the diagonal tend towards zero: this means that the eigenvectors show less similarities between each other, facilitating their interpretation.
.

Mode	PROM frequency [Hz]	FEM frequency [Hz]	Percentage error [%]
1	164.9	164.9	0.00
2	552.1	552.1	0.00
3	774.8	774.8	0.00
4	1337.3	1337.3	0.00
5	3210.0	3210.0	0.00
6	3861.1	3861.4	-0.01
7	4519.6	4519.5	0.00
8	5100.2	5100.3	0.00
9	6563.3	6564.1	-0.01
10	6917.2	6917.1	0.00
11	7336.7	7336.7	0.00
12	7695.2	7695.8	-0.01
13	8564.2	8564.4	0.00
14	9150.0	9150.4	-0.01
15	10348	10348	0.01
16	12006	12007	0.00
17	12122	12123	0.00
18	14238	14238	0.01
19	15090	15090	0.01
20	16267	16270	-0.02

Table 3.15: Natural frequencies comparison, Blade, Eigenvalues and eigenvectors interpolation VS Full reference model, 5.14 mm, $\Delta p = 0.1$ mm
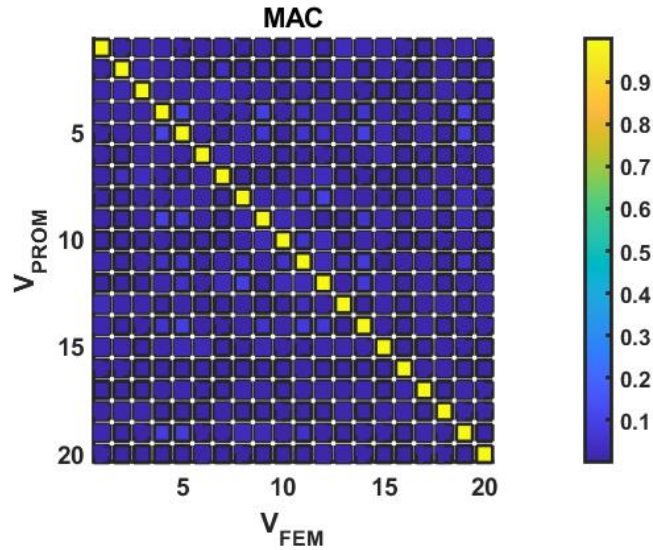
Figure 3.49: MAC, Blade, Eigenvalues and eigenvectors interpolation VS Full reference model, 5.14 mm, 20 modes

For what concerns the forced response, the details about how it was conducted have already been explained in the previous paragraphs: here we find the figure referring to the comparison between the two models, in particular with a focus on the 1st mode solicitation. The results are excellent, since the overlapping between the two curves is completely reached and the error between the peak amplitudes is negligible.
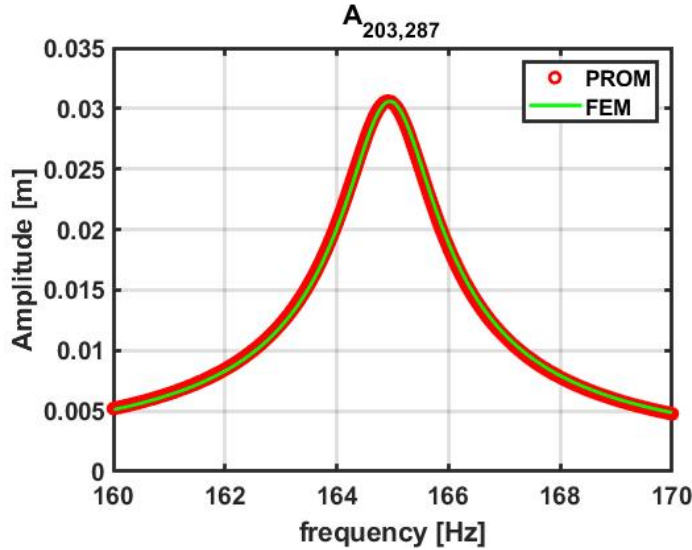

Figure 3.50: Forced response, Blade, Eigenvalues and eigenvectors interpolation VS Full reference model, 5.14 mm

A further validation has been carried out comparing the peak amplitudes at every master degree of freedom with respect to each other, both in the PROM and in the reference FEM models. For sake of brevity these results are not reported explicitly, but they confirm that the method guarantees an optimal approximations, at least for what concerns the master degrees of freedom. Finally, the matrix mapping manifest a behaviour which is identical to the previous cantilever beam case: while the matrices of the 5 stations' reduced order models have the typical Craig-Bampton CMS conformation, the interpolated matrices are full, and the terms inside them do not show any specific correlation. This is the main drawback of the method, especially because the full matrices have an higher computational cost; however, if the reduction is efficiently performed, the dimension of the reduced order model makes it easy to handle, independently from the matrices' mapping.

If now we consider the second wider pattern, characterized by a value of $\Delta p = 0.2$ mm, our reference model is now located between the 3rd and the 4th stations, exactly where the eigenvector exchange occurred. Therefore, it is interesting to see the difference between the results without the preliminary modes' sorting and the outcomes after the rearrangement. The two situations are illustrated in the figures 3.52 and 3.51, which show the MAC comparison of the two interpolated models against the reference one.
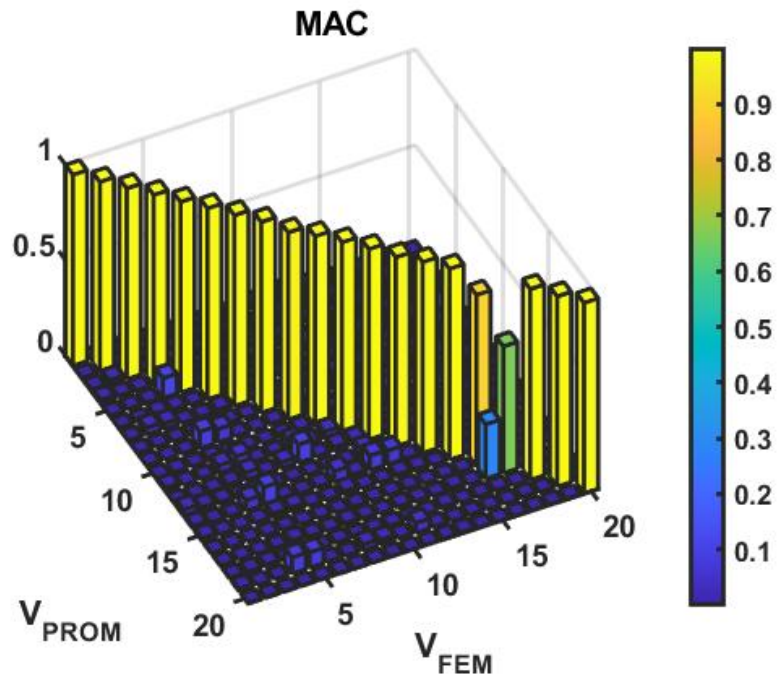
Figure 3.51: MAC, Blade, Eigenvalues and Eigenvectors interpolation VS full reference model, 5.14 mm, without eigenvectors sorting
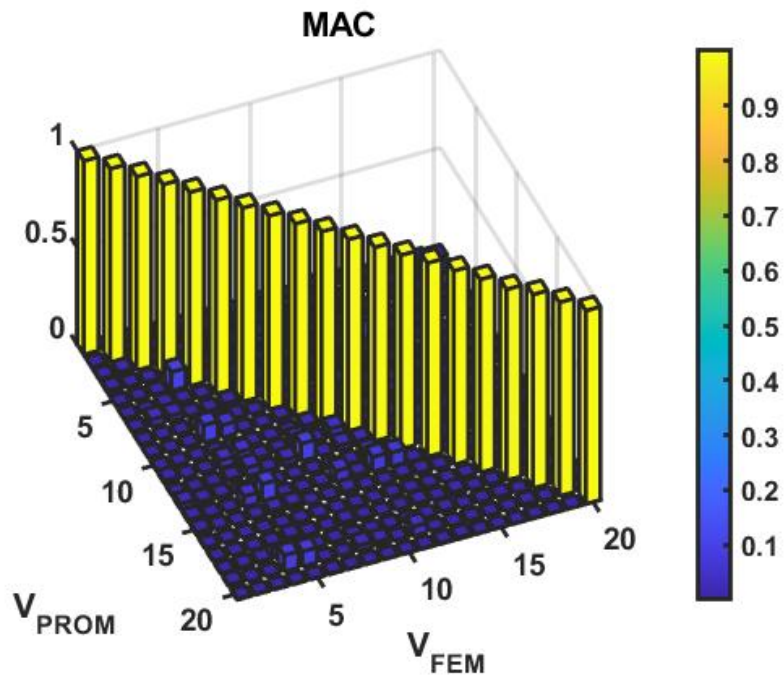
Figure 3.52: MAC, Blade, Eigenvalues and Eigenvectors interpolation VS full reference model, 5.14 mm, with eigenvectors sorting

From the previous figures it is evident that the eigenvectors rearrangement is necessary to avoid bad quality approximations in correspondence of exchanging modes. After having performed this operation, even the percentage errors on natural frequencies can be computed, showing slightly higher values with respect to the previous tight pattern (table 3.16).

Mode	PROM frequency [Hz]	FEM frequency [Hz]	Percentage error [%]
1	165	164.9	0.06
2	552.0	552.1	-0.02
3	774.9	774.8	0.01
4	1337.4	1337.3	0.01
5	3209.8	3210.0	0.01
6	3860.9	3861.4	-0.01
7	4519.8	4519.5	0.01
8	5100.3	5100.3	0.00
9	6562.3	6564.1	-0.03
10	6917.6	6917.1	0.01
11	7336.5	7336.7	0.00
12	7695.2	7695.8	-0.01
13	8562.9	8564.4	-0.02
14	9149.9	9150.4	-0.01
15	10349	10348	0.01
16	12007	12007	0.00
17	12121	12123	-0.02
18	14238	14238	0.00
19	15090	15090	0.00
20	16254	16270	-0.09

Table 3.16: Natural frequencies comparison, Blade, Eigenvalues and eigenvectors interpolation VS Full reference model, 5.14 mm, $\Delta p = 0.2$ mm

.

Conclusions

This thesis presented the implementation of three selected interpolation techniques applied to different type of systems, characterized by the variation of one geometrical parameter. In particular, the objective was to find an effective procedure suitable for the application on reduced order models, obtained through the Craig-Bampton Component Mode Synthesis. Starting from a simple One-dimensional model, many simulations have been carried out, highlighting the main drawbacks encountered. Observing firstly the results of the 1D full system section, all the methods manifested an optimal accuracy in predicting the natural frequencies, the modeshapes and the linear forced response; however, when the CB-CMS reduction was introduced many problems arise: for example, the element by element interpolation expressed the occurrence of complex modes, related to the fact that the interpolated mass matrix was not positive definite. Similarly, the Taylor series interpolation with the derivatives approximated by means of finite differences terms showed quite good results in proximity of the nominal station, while it was affected by complex modes presence when moving away from it. The only technique that provided good results in relation to reduced order models is the interpolation of eigenvalues and eigenvectors: it has been conceived appositely to avoid the outbreak of complex modes and has shown positive results also for the other 3D models tested. In detail, this technique has allowed to obtain negligible percentage errors in the comparison with the reference natural frequencies and it has also proven to be suitable for the simulation of structures characterized by exchanges in consecutive eigenvectors' position along the stations, thanks to a preliminary sorting procedure. In fact the MAC plots generated with this technique have always been close to the ideal diagonal shape and for what concerns the forced response the match obtained through the mode superposition has been more than acceptable in all the simulated cases, considering mainly the master degrees of freedom. On the other hand the principal drawback is represented by the resulting matrices' mapping, that is not comparable with the typical CB-CMS reduced order model matrices' conformation. Independently from this aspect, it is also necessary to remind that the method has been tested on models with a simplified geometry, and for this reason it should be applied also to more articulated system, as for example a real blade profile, before being completely approved. If this further validation was successful, then the application to a full bladed disk characterize by different blades in order to simulate the effect of geometrical mistuning would be possible.

Bibliography

[1] Sung-Kwon Hong, BogdanI.Epureanu, MatthewP.Castanier, DavidJ.Gorsich , *Parametric reduced-order models for predicting the vibration response of complex structures with component damage and uncertainties*, Journal of Sound and Vibration (2010)

[2] Eric Kurstak, Ryan Wilber, Kiran D'Souza, *Parametric reduced order models for bladed disks with mistuning and varying operational speed*, Journal of Engineering for Gas Turbines and Power (2018)

[3] Eric Kurstak, Kiran D'Souza, *Forced response computation for bladed disks industrial practices and advanced methods*, AIAA Journal (2020)

[4] E.Senturier, *Experimental investigation of bladed disk dynamics at design speed under synchronous vibration*, Turbomeca (SAFRAN) (2007)

[5] Gilbert Strang, *Introduction to linear algebra, fifth edition*, Massachusetts Institute of Technology (2016)

[6] Marco Mazzucco, *Parametric model order reduction by matrix interpolation on lie groups*, Tesi di dottorato, Politecnico di Torino (2014)

[7] A. Fasana, S. Marchesiello, *Meccanica delle vibrazioni*, CLUT (2006)

[8] Giancarlo Genta, *Vibration Dynamics and Control*, Springer (2009)

[9] Stefano Zucca, *Slides del corso di "Dinamica dei rotori per applicazioni aerospaziali"*, (2021)

Appendix A.

Mesh Morphing

The mesh morphing is a specific method that allows to modify the mesh of a FEM model, without changing the numeration of nodes and elements. In this thesis work it turned out to be a valuable tool, in particular with reference to the dummy blade modeling, since it enabled to realize the mesh only once, in correspondence of the nominal station, and then create the other four station and the perturbed conditions by means of slight displacements imposed on some nodes. The whole procedure has allowed to save much time and was entirely performed into the software Hypermesh. It is important to underline that this appendix is not an exhaustive description of the mesh morphing tool, since this latter has been applied to a simplified geometry in correspondence of planar faces: for this reason, further and advanced procedures are not faced here.

First of all, the 3D model has to be meshed properly, avoiding distorted elements and merging the nodes where required. After that, if the solid mapping procedure has been followed, it is necessary to delete the starting 2D meshed surfaces and leave only the 3D elements in the model. This passage can be performed by means of the following commands: *Tool > delete > elems > by geoms > surfs*.
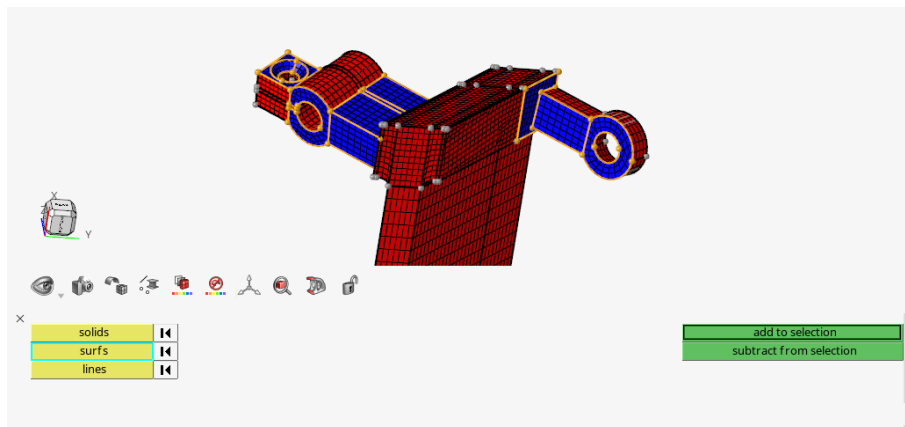
Figure A.1: Selection of the 2D mesh surfaces to delete

After this step it is also convenient to collect the elements that will be subjected to the mesh morphing procedure into single colored components, in order to facilitate their selection. This passage can be done through the commands *Tool > organize > includes > elems > dest*. An example of components subdivision is reported in figure A.4. Now the mesh morphing can be implemented, as represented in the next picture: inside the Morph section, selecting "Free", a window with *Move*, *Targets*, *Anchors* and *MorphArea* opens.
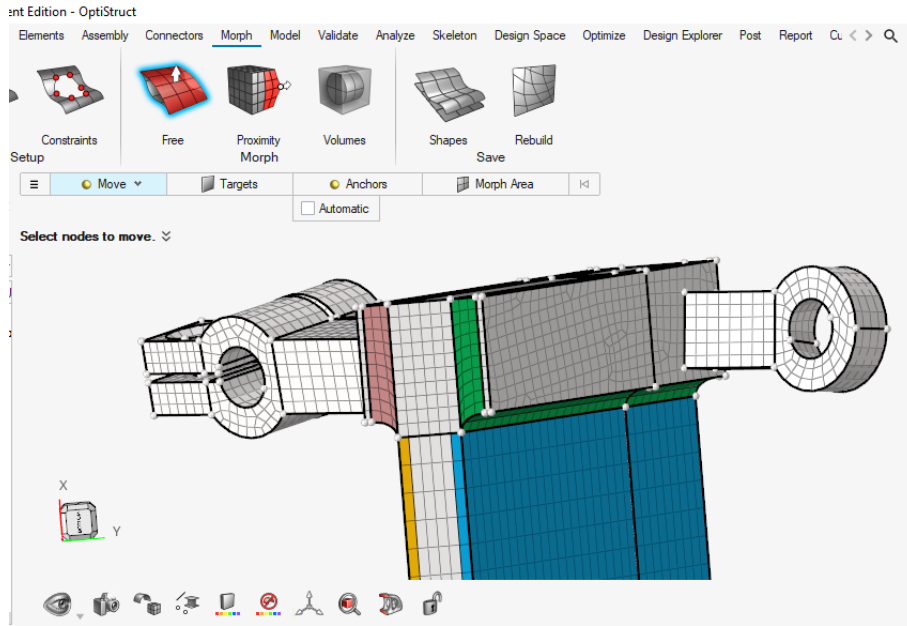

Figure A.2: Morph, Free

If we choose to move the nodes of the main body of the blade, then we must select them by means of *Move >* right-click *> Select > By Face* and then choose the desired surface on which they are present (figure A.3). Then, *Morph-area >* right-click *> Select > By component* and choose the elements that will be affected by the displacements of the moving nodes. In the blade case, since the movement is imposed to the nodes on the blue planar surface of the main body, the morph area selected includes only the upper part colored in green and the lower part colored in purple (figure A.4).
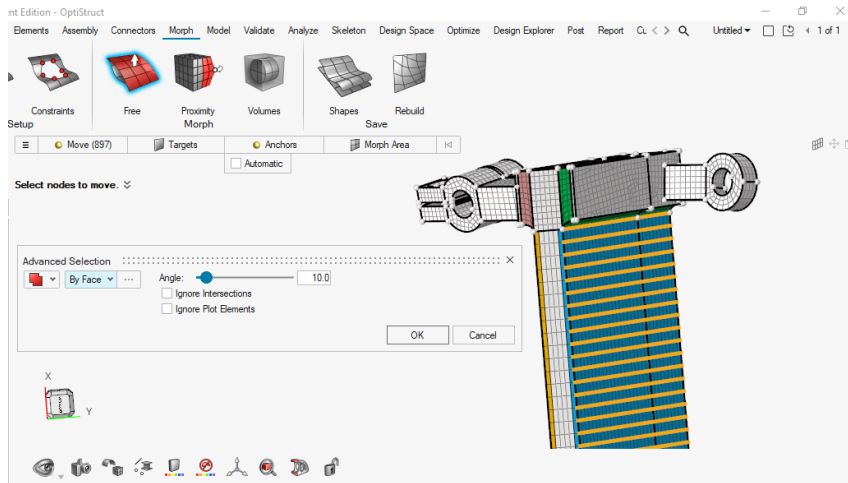
Figure A.3: Moving nodes selection
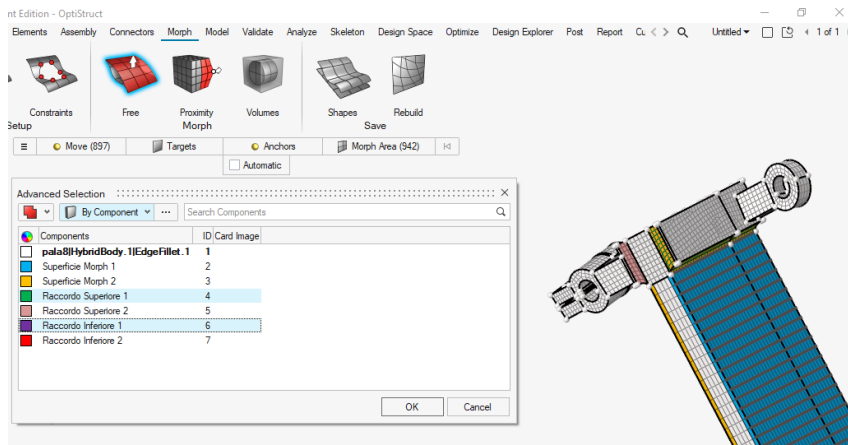
Figure A.4: MorphArea selection

Subsequently, a reference system appears and allows to choose in which direction operate the node movement. In order to create a new shape, click on the record button (figure A.5) then click on the Y arrow, where it is possible to insert the value of the displacement assigned to the selected nodes (figure A.6), and finally click on the plus symbol to create the morphed shape (figure A.5).

Once the shape is created, it is possible to find it in the shape menu, where it can be previewed or applied permanently to the model (figure A.7). There is also the possibility to apply simultaneously multiple shapes, as was done for the blade model, since for each station 2 shapes relative to the displacement of opposite main body faces' nodes were required.

Finally, once a shape is saved and applied to the model, the file can be exported in .bdf format in order to be compatible with the software Ansys APDL, where the material is assigned and all the simulations are performed.
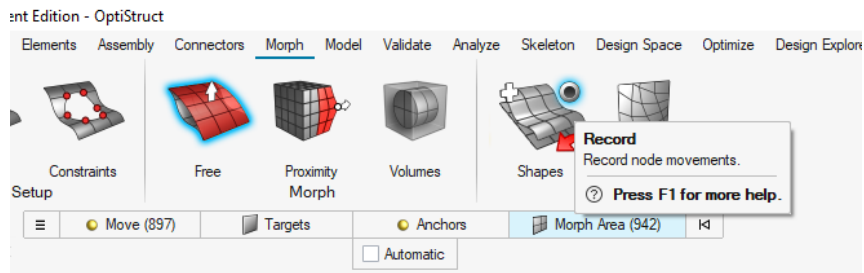
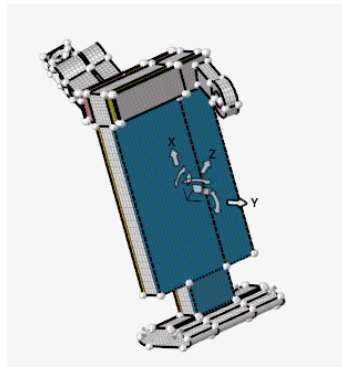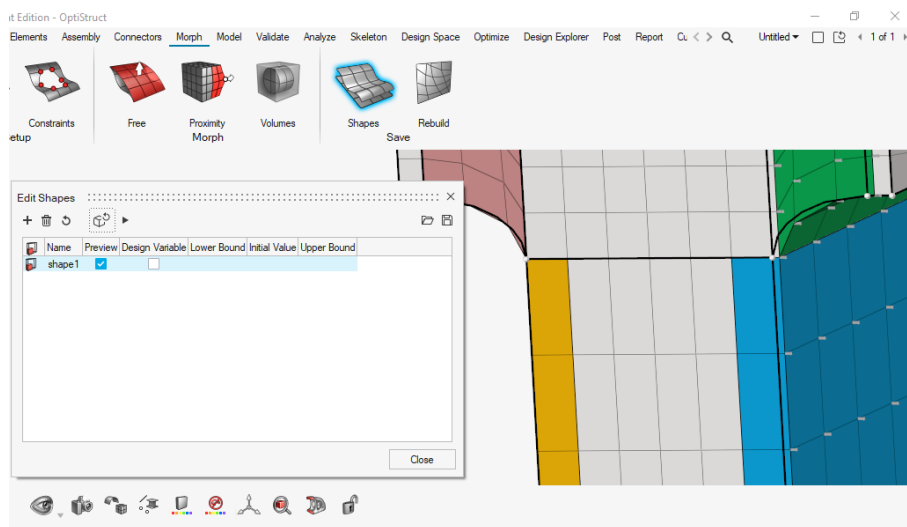**Figure A.5:** Shape recording and creation

Figure A.6: Displacement direction

Figure A.7: Shapes menu and mesh morphing result